Effective interface conditions for the forced infiltration of a viscous fluid into a porous medium using homogenization

Thomas Carraro[a,1], Christian Goll[a], Anna Marciniak-Czochra[a,b,2], Andro Mikelić[c,3,*]

[a] *Institute for Applied Mathematics, Heidelberg University, 69120 Heidelberg, Germany*
[b] *Bioquant, Heidelberg University, 69120 Heidelberg, Germany*
[c] *Université de Lyon, Lyon, F-69003, France; Université Lyon 1, Institut Camille Jordan, UMR 5208, Bât. Braconnier, 43, Bd du 11 novembre 1918, 69622 Villeurbanne Cedex, FRANCE*

Abstract

It is generally accepted that the effective velocity of a viscous flow over a porous bed satisfies the Beavers-Joseph slip law. To the contrary, in the case of a forced infiltration of a viscous fluid into a porous medium the interface law has been a subject of controversy. In this paper, we prove rigorously that the effective interface conditions are: (i) the continuity of the normal effective velocities; (ii) zero Darcy's pressure and (iii) a given slip velocity. The effective tangential slip velocity is calculated from the boundary layer and depends only on the pore geometry. In the next order of approximation, we derive a pressure slip law. An independent confirmation of the analytical results using direct numerical simulation of the flow at the microscopic level is given, as well.

This paper is dedicated to Mary F. Wheeler, as a tribute for her impact on introducing mathematical rigour to realistic porous media problems.

To appear in **Computer Methods in Applied Mechanics and Engineering**, 2014, doi: 10.1016/j.cma.2014.10.050

[*] Corresponding author

Email addresses: thomas.carraro@iwr.uni-heidelberg.de (Thomas Carraro), christian.goll@iwr.uni-heidelberg.de (Christian Goll), anna.marciniak@iwr.uni-heidelberg.de (Anna Marciniak-Czochra), mikelic@univ-lyon1.fr (Andro Mikelić)

[1] TC was supported by the German Research Council (DFG) through project "Modellierung, Simulation und Optimierung der Mikrostruktur mischleitender SOFC-Kathoden" (RA 306/17-2).

[2] AM-C was supported by ERC Starting Grant "Biostruct" No. 210680 and Emmy Noether Programme of German Research Council (DFG).

[3] The research of A.M. was partially supported by the Programme Inter Carnot Fraunhofer from BMBF (Grant 01SF0804) and ANR. Research visits of A.M. to the Heidelberg University were supported in part by the Romberg professorship at IWR, Heidelberg University, 2011-1013.

Keywords: Interface conditions, pore scale simulation, pressure slip law, slip velocity, boundary layers, homogenization
2000 MSC: 35Q35, 35B27, 76S05, 76D10, 65Z05

1. Introduction

The aim of this paper is to derive rigorously interface conditions governing the infiltration of a viscous fluid into a porous medium.

We start from an incompressible 2D flow of a Newtonian fluid penetrating a porous medium. At the pore scale, the flow is described by the stationary Stokes system, both, in the unconstrained fluid part and in the pore space. Upscaling of the Stokes system in a porous medium yields Darcy's law as the effective momentum equation, valid at every point of the porous medium. The two models, Stokes system and the Darcy equation, are partial differential equations of different order and need to be coupled at the interface of the fluid and the porous medium. The resulting system should provide an approximation of the starting first principles with error estimate in the term of the dimensionless pore size ε, being the ratio of the characteristic pore size and the macroscopic domain length.

The main result of this paper is a rigorous derivation of the effective filtration equation and the interface condition from the pore scale level description based on first principles, supported by a direct pore scale simulation of the Stokes equations.

The resulting interface conditions take the form:

(i)

$$u_2^{eff} = u_2^D \quad \text{and} \quad P^D = 0 \quad \text{on} \quad \{x_2 = 0\}, \tag{1}$$

where $\{\mathbf{u}^D, P^D\}$ are the Darcy velocity and the pressure and $\mathbf{u}^{eff}$ is the unconfined fluid velocity.

(ii)

$$u_1^{eff} = C_1^{2,bl} \frac{\partial P^D}{\partial x_2} \quad \text{on} \quad \{x_2 = 0\}, \tag{2}$$

where $C_1^{2,bl}$ is a boundary layer stabilization constant given by (11). Note that in general $C_1^{2,bl} \neq K_{12}$ K being the permeability tensor, and there is a jump of the effective tangential velocities.

There is vast literature on modeling interface conditions between a free flow and a porous medium. Most of the references focus on flows which are tangential to the porous medium. In such situation, the free fluid velocity is much larger than the Darcy velocity in the porous medium. The corresponding interface condition is the slip law by Beavers and Joseph. It was deduced from the experiment in [3], then discussed and simplified into a generally used form in [30] and justified through numerical simulations of pore level Navier-Stokes equations in [31], [20] and [7]. A rigorous justification of the slip law by Beavers and Joseph, starting from the pore level first principles, was provided by Jäger and Mikelić in [17], using a combination of homogenization and boundary layers techniques. The slip law is supplemented by the pressure jump law, what was noticed in [18] and rigorously derived in [25]. A corresponding numerical validation by solving the Stokes equation at the pore scale has been recently presented in [7].

Infiltration into a porous medium corresponds to a different situation, in which the free fluid velocity and the Darcy velocity are of the same order. We refer to the article by Levy and Sanchez-Palencia [23]. They classify the physical situation as "Case B: The pressure gradient on the side of the porous body at the interface is normal to it". In the "Case B" the pressure gradient in the porous medium is much larger than in the free fluid. Using an order-of-magnitude analysis, in [23] it was concluded that the effective interface conditions have to satisfy conditions (1). Note that the interface conditions (1) were obtained for low Reynolds number flows.

In order to close the system, one more condition is needed. In [23] an intermediate boundary layer was introduced and existence of an effective slip velocity at the interface was postulated. However, the article [23] did not provide the slip velocity. It was limited to a model of macroscopic isotropy, where the slip is equal to zero. Therefore, zero tangential velocity was assumed.

A rigorous mathematical study of the interface conditions between a free fluid and a porous medium was initiated in [16]. Our analysis reposes on the boundary layers constructed there. For reviews of the models and techniques we refer to [11] and [19].

We note that in a number of articles devoted to numerical simulations, the porous part was modeled using the Brinkman-extended Darcy law. We refer to [10], [13], [14], [26], [35] and references therein. In such setting, the authors used general interface conditions introduced by Ochoa-Tapia and Whitaker in [28]. They consist of (i) continuity of the velocity and (ii) complex jump relations for the stresses, containing several parameters to be fitted. We recall that the viscosity in the Brinkman equation is not known and the use of it seems to be justified only in the case of a high porosity (see the discussion in [27]). Furthermore, Larson and Higdon undertook a detailed numerical simulation of two configurations (axial and transverse) of a shear flow over a porous medium in [21]. Their conclusion was that a macroscopic model based on Brinkman's equation gives "reasonable predictions for the rate of decay of the mean velocity for certain simple geometries, but fails for to predict the correct behavior for media anisotropic in the plane normal to the flow direction". An approach using the thermodynamically constrained averaging theory was presented in [15]. Darcy-Navier-Stokes coupling yields also interesting numerical problems, see [22], [29] and [11] and references therein.

In our work we use a finite element method to obtain a numerical confirmation of the analytical results. Numerical study of the convergence rates of the macroscopic problems and effective interface conditions is a challenging task. The first difficulty is to find a numerical solution of the microscopic problem used as a reference. The geometry of the porous part has to be resolved with high accuracy. In addition, the microscopic solution in the vicinity of the surface of the porous medium has large gradients that can be approximated only by a boundary layer, as shown in this work. The accuracy needed by the resolution of the interface and porous part requires high performance computing. In our test cases, we reduce the computational costs by considering a problem with periodic geometry and periodic boundary conditions. Thus, we reduce the computations to one column of inclusions in the porous part. Nevertheless, even in the simplified example problem all the computations must be performed with high accuracy. The reason is that the homogenization errors, especially in the estimates based on correction terms, are small in comparison with numerical errors even for simulations with millions of degrees of freedom. A further difficulty is that to check the estimates numerically, we have to solve several auxiliary problems which are coupled. Therefore the numerical precision of one problem influences the precision of the other ones. Due to the complexity of the microscopic flow and the boundary layers, strategies for local mesh adaptivity to reduce the computations of the norms in the estimates are not effective. We nevertheless apply a goal oriented adaptive method, based on the dual weighted residual (DWR) method [4], to calculate some constants needed for the estimates, increasing the overall accuracy of our numerical tests.

The paper is organized as follows: In Section 2 we formulate the microscopic problem and the resulting effective equations. We provide theorems on error estimates of the model approximation. In Section 3 we give a numerical confirmation of the analytical results based on finite element computations. Sections 4–5 contain the corresponding proofs. The necessary results on boundary layers and very weak solutions to the Stokes system will be recalled in the proofs of the main results.

2. Problem setting and main results

2.1. Definition of the geometry

Let L, h and H be positive real numbers. We consider a two dimensional periodic porous medium $\Omega_2 = (0, L) \times (-H, 0)$ with a periodic arrangement of the pores. The

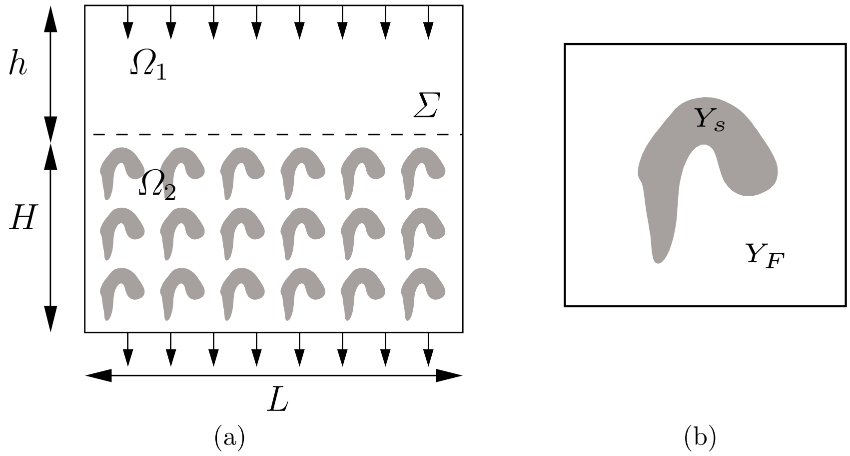

Figure 1: Sketch of the geometry (a) the periodicity cell Y (b).

formal description goes along the following lines:

First, we define the geometrical structure inside the unit cell $Y = (0,1)^2$. Let Y_s (the solid part) be a closed strictly included subset of $\bar{Y}$, and $Y_F = Y \backslash Y_s$ (the fluid part). Now we make a periodic repetition of Y_s all over $\mathbb{R}^2$ and set $Y_s^k = Y_s + k$, $k \in \mathbb{Z}^2$. Obviously, the resulting set $E_s = \bigcup_{k \in \mathbb{Z}^2} Y_s^k$ is a closed subset of $\mathbb{R}^2$ and $E_F = \mathbb{R}^2 \backslash E_s$ in an open set in $\mathbb{R}^2$. We suppose that Y_s has a boundary of class C^∞, which is locally located on one side of their boundary. Obviously, E_F is connected and E_s is not.

Now we notice that Ω_2 is covered with a regular mesh of size ε, each cell being a cube Y_i^ε, with $1 \le i \le N(\varepsilon) = |\Omega_2|\varepsilon^{-2}[1 + o(1)]$. Each cube Y_i^ε is homeomorphic to Y, by linear homeomorphism Π_i^ε, being composed of translation and a homothety of ratio $1/\varepsilon$.

We define $Y_{S_i}^\varepsilon = (\Pi_i^\varepsilon)^{-1}(Y_s)$ and $Y_{F_i}^\varepsilon = (\Pi_i^\varepsilon)^{-1}(Y_F)$. For sufficiently small $\varepsilon > 0$ we consider the set $T_\varepsilon = \{k \in \mathbb{Z}^2 | Y_{S_k}^\varepsilon \subset \Omega_2\}$ and define

$$O_\varepsilon = \bigcup_{k \in T_\varepsilon} Y_{S_k}^\varepsilon, \quad S^\varepsilon = \partial O_\varepsilon, \quad \Omega_2^\varepsilon = \Omega_2 \backslash O_\varepsilon = \Omega_2 \cap \varepsilon E_F$$

Obviously, $\partial \Omega_2^\varepsilon = \partial \Omega_2 \cup S^\varepsilon$. The domains O_ε and Ω_2^ε represent, respectively, the solid and fluid parts of the porous medium Ω. For simplicity, we suppose $L/\varepsilon, H/\varepsilon, h/\varepsilon \in \mathbb{N}$.

We set $\Sigma = (0, L) \times \{0\}$, $\Omega_1 = (0, L) \times (0, h)$ and $\Omega = (0, L) \times (-H, h)$. Furthermore, let $\Omega^\varepsilon = \Omega_2^\varepsilon \cup \Sigma \cup \Omega_1$ and $\Omega = \Omega_2 \cup \Sigma \cup \Omega_1$. (See Fig. 1a)

2.2. The microscopic model

Having defined the geometrical structure of the porous medium, we precise the flow problem.

We consider the slow viscous incompressible flow of a single fluid through a porous medium. The flow is caused by the fluid injection at the boundary $\{x_2 = h\}$. We suppose the no-slip condition at the boundaries of the pores (i.e. the filtration through a rigid porous medium). Then, the flow is described by the following non-dimensional steady Stokes system in Ω^ε (the fluid part of the porous medium Ω):

$$-\Delta \mathbf{v}^\varepsilon + \nabla p^\varepsilon = 0 \qquad \text{in} \quad \Omega^\varepsilon, \tag{3a}$$

$$\text{div } \mathbf{v}^\varepsilon = 0 \qquad \text{in} \quad \Omega^\varepsilon, \qquad \int_{\Omega_1} p^\varepsilon \, dx = 0, \tag{3b}$$

$$\mathbf{v}^\varepsilon = 0 \quad \text{on} \quad \partial\Omega^\varepsilon \setminus \Omega, \qquad \{\mathbf{v}^\varepsilon, p^\varepsilon\} \quad \text{is } L - \text{periodic in } \ x_1, \tag{3c}$$

$$\mathbf{v}^\varepsilon|_{x_2=h} = \mathbf{v}^D, \quad v_2^\varepsilon|_{x_2=-H} = g, \quad \frac{\partial v_1^\varepsilon}{\partial x_2}|_{x_2=-H} = 0. \tag{3d}$$

Such flow is possible only under the following compatibility condition

$$LU_B = \int_0^L g(x_1)\, dx_1 = \int_0^L v_2^D(x_1)\, dx_1. \tag{4}$$

With the assumption on the geometry from section 2.1, condition (4) and for $\mathbf{f} \in C^\infty(\overline{\Omega})^2$, $\mathbf{v}^D \in C^\infty[0,L]^2$ and $g \in C^\infty[0,L]$, problem (3a)-(3d) admits a unique solution $\{\mathbf{v}^\varepsilon, p^\varepsilon\} \in C^\infty(\overline{\Omega^\varepsilon})^3$, for all $\varepsilon > 0$.

Our goal is to study behavior of solutions to system (3a)-(3d), when $\varepsilon \to 0$. In such limit the equations in Ω_1 remain unchanged and in Ω_2^ε the Stokes system is upscaled to Darcy's equation posed in Ω_2. Our contribution is the derivation of the interface condition, linking these two systems.

2.3. The boundary layers and effective coefficients

Let the permeability tensor K be given by

$$K_{ij} = \int_{Y_F} \nabla_y \mathbf{w}^i : \nabla_y \mathbf{w}^j \, dy = \int_{Y_F} w_j^i \, dy, \ 1 \le i,j \le 2. \tag{5}$$

where for $1 \le i \le 2$, $\{\mathbf{w}^i, \pi^i\} \in H^1_{per}(Y_F)^2 \times L^2(Y_F)$, $\int_{Y_F} \pi^i(y)\, dy = 0$, are solutions to

$$\begin{cases} -\Delta_y \mathbf{w}^i(y) + \nabla_y \pi^i(y) = \mathbf{e}^i & \text{in } \ Y_F \\ \text{div}_y \mathbf{w}^i(y) = 0 & \text{in } \ Y_F \\ \mathbf{w}^i(y) = 0 & \text{on } \ (\partial Y_F \setminus \partial Y). \end{cases} \tag{6}$$

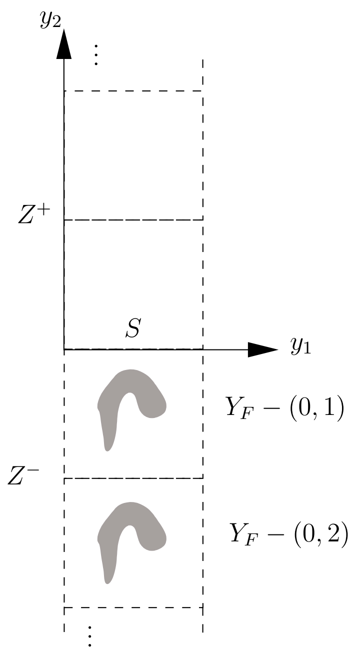

Figure 2: The boundary layer geometry

(See Fig. 1b). Obviously, these problems always admit unique solutions and K is a symmetric positive definite matrix (the dimensionless permeability tensor). In addition

$$K_{j2} = K_{2j} = \int_0^1 w_2^j(y_1, 0)\ dy_1. \tag{7}$$

In order to formulate the result we need the viscous boundary layer problem connecting free fluid flow and a porous medium flow:

In the Fig. 2, the interface is $S = (0,1) \times \{0\}$, the free fluid slab is $Z^+ = (0,1) \times (0, +\infty)$ and the semi-infinite porous slab is $Z^- = \cup_{k=1}^{\infty}(Y_F - \{0,k\})$, where $Y_F - \{0,k\}$ denotes the translation of the pore Y_F for k in the negative y_2 direction. The flow region is then $Z_{BL} = Z^+ \cup S \cup Z^-$.

We consider the following problem:

Find $\{\beta^{j,bl},\omega^{j,bl}\}$, $j=1,2$, with square-integrable gradients satisfying

$$-\Delta_y \beta^{j,bl}+\nabla_y \omega^{j,bl}=0 \qquad \text{in } Z^+\cup Z^- \tag{8a}$$
$$\operatorname{div}_y \beta^{j,bl}=0 \qquad \text{in } Z^+\cup Z^- \tag{8b}$$
$$\big[\beta^{j,bl}\big]_S(\cdot,0)=K_{2j}\mathbf{e}^2-\mathbf{w}^j \quad \text{on } S \tag{8c}$$
$$\big[\{\nabla_y\beta^{j,bl}-\omega^{j,bl}I\}\mathbf{e}^2\big]_S(\cdot,0)=-\{\nabla_y\mathbf{w}^j-\pi^j I\}\mathbf{e}^2 \;\text{ on } S \tag{8d}$$
$$\beta^{j,bl}=0 \quad \text{on } \cup_{k=1}^{\infty}\left(\partial Y_s-\{0,k\}\right), \qquad \{\beta^{j,bl},\omega^{j,bl}\} \text{ is } 1-\text{periodic in } y_1. \tag{8e}$$

By Lax-Milgram's lemma, there exists a unique $\beta^{j,bl}\in L^2_{loc}(Z_{BL})^2$, $\nabla_y\beta^{j,bl}\in L^2(Z^+\cup Z^-)^4$ satisfying (8a)-(8e) and $\omega^{j,bl}\in L^2_{loc}(Z_{BL})$, which is unique up to a constant and satisfying (8a). After the results from [16], the system (8a)-(8e) describes a boundary layer, i.e. $\beta^{j,bl}$ and $\omega^{j,bl}$ stabilize exponentially towards constants, when $|y_2|\to\infty$: There exist $\gamma_0>0$ and $\mathbf{C}^{j,bl}$ and C^j_π such that

$$|\beta^{j,bl}-\mathbf{C}^{j,bl}|+|\omega^{j,bl}-C^j_\pi|\le Ce^{-\gamma_0 y_2}, \qquad y_2>0, \tag{9}$$
$$e^{-\gamma_0 y_2}\nabla_y\beta^{j,bl}, \quad e^{-\gamma_0 y_2}\beta^{j,bl}, \quad e^{-\gamma_0 y_2}\omega^{j,bl}\in L^2(Z^-), \tag{10}$$
$$\mathbf{C}^{j,bl}=(C_1^{j,bl},0)=\Big(\int_S \beta_1^{j,bl}(y_1,+0)\,dy_1,0\Big), \tag{11}$$
$$C^j_\pi=\int_0^1 \omega^{j,bl}(y_1,+0)\,dy_1. \tag{12}$$

The case $j=2$ is of special importance. If we suppose the mirror symmetry of the solid obstacle Y_s with respect to y_1, then it is easy to prove that w_1^2 is uneven in y_1 with respect to the line $\{y_1=1/2\}$, and w_2^2 and π^2 are even. Consequently, $K_{12}=K_{21}=0$ and the permeability tensor K is diagonal. Next we see that $\beta_1^{2,bl}$ is uneven in y_1 with respect to the line $\{y_1=1/2\}$, and $\beta_2^{2,bl}$ and ω^2 are even. Using formula (11) yields $C_1^{2,bl}=0$ in the case of the mirror symmetry of the solid obstacle Y_s with respect to y_1.

2.4. The macroscopic model

Now we introduce the effective problem in Ω. It consists of two problems, which are to be solved sequentially. The first problem is posed in Ω_2 and reads:

Find a pressure field P^D which is the $L-$ periodic in x_1 function satisfying

$$\mathbf{u}^D=-K\nabla P^D \quad \text{and} \quad \operatorname{div}\Big(K\nabla P^D\Big)=0 \;\text{ in }\; \Omega_2 \tag{13a}$$
$$P^D=0 \;\text{ on }\; \Sigma; \quad -K\nabla P^D|_{\{x_2=-H\}}\cdot\mathbf{e}^2=g. \tag{13b}$$

We note that the value $P^D|_\Sigma$ of pressure field at the interface Σ is equal to zero.

Problem (13a)-(13b) admits a unique solution $\{\mathbf{u}^D, P^D\} \in C^\infty(\overline{\Omega}_2)^3$.

Next, we study the situation in the unconfined fluid domain Ω_1:

Find a velocity field $\mathbf{u}^{eff}$ and a pressure field p^{eff} such that

$$-\triangle \mathbf{u}^{eff} + \nabla p^{eff} = 0 \qquad \text{in } \Omega_1, \tag{14a}$$

$$\text{div } \mathbf{u}^{eff} = 0 \qquad \text{in } \Omega_1, \qquad \int_{\Omega_1} p^{eff}\, dx = 0, \tag{14b}$$

$$\mathbf{u}^{eff} = \mathbf{v}^D \qquad \text{on } (0,L)\times\{h\}; \quad \mathbf{u}^{eff} \text{ and } p^{eff} \quad \text{are } L-\text{periodic in} \quad x_1, \tag{14c}$$

$$u_2^{eff} = -K\nabla P^D \cdot \mathbf{e}^2 = -K_{22}\frac{\partial P^D}{\partial x_2} \qquad \text{and} \qquad u_1^{eff} = C_1^{2,bl}\frac{\partial P^D}{\partial x_2} \qquad \text{on} \quad \Sigma. \tag{14d}$$

The constant $C_1^{2,bl}$ is given by (11) and requires solving problem (8a)-(8e).

Again, using the compatibility condition (4) we obtain easily that problem (14a)-(14d) has a unique solution $\{\mathbf{u}^{eff}, p^{eff}\} \in C^\infty(\overline{\Omega}_1)^3$.

2.5. The main result

In this section we formulate the approximated model. We expect that the Stokes system remains valid in Ω_1.

Since $U_B = O(1) \neq 0$, the filtration velocity has to be of order $O(1)$. Therefore, after [1], [19] and [32], the asymptotic behavior of the velocity and pressure fields in the porous part Ω_2, in the limit $\varepsilon \to 0$, is given by the two-scale expansion

$$\mathbf{v}^\varepsilon \approx \mathbf{u}^0(x,y) + \varepsilon \mathbf{u}^1(x,y) + O(\varepsilon^2), \quad y = \frac{x}{\varepsilon},$$
$$p^\varepsilon \approx \frac{1}{\varepsilon^2}P^D(x) + \frac{1}{\varepsilon}p^1(x,y) + O(1), \quad y = \frac{x}{\varepsilon},$$
$$\mathbf{u}^0(x,y) = -\sum_{j=1}^{2} \mathbf{w}^j(y)\frac{\partial P^D(x)}{\partial x_j}, \quad p^1(x,y) = -\sum_{j=1}^{2} \pi^j(y)\frac{\partial P^D(x)}{\partial x_j}.$$

The boundary layers given by (8a)-(8e) will be used to link the above approximation on Σ with the solution of the Stokes system. With such strategy, at the main order approximation reads

$$\mathbf{v}^\varepsilon = H(x_2)(\mathbf{u}^{eff} - C_1^{2,bl}\frac{\partial P^D}{\partial x_2}|_\Sigma \mathbf{e}^1) - H(-x_2)\sum_{k=1}^{2}\frac{\partial P^D}{\partial x_k}\mathbf{w}^k(\frac{x}{\varepsilon}) +$$
$$\frac{\partial P^D}{\partial x_2}|_\Sigma \beta^{2,bl}(\frac{x}{\varepsilon}) + O(\varepsilon) + \text{ outer boundary layer,} \tag{15}$$
$$p^\varepsilon = H(x_2)p^{eff} + H(-x_2)\{\varepsilon^{-2}P^D - \frac{1}{\varepsilon}\sum_{k=1}^{2}(\frac{\partial P^D}{\partial x_k}\pi^k(\frac{x}{\varepsilon}) + \mathcal{A}_\pi^k \delta_{2k})\} +$$
$$\frac{1}{\varepsilon}(\omega^{2,bl}(\frac{x}{\varepsilon}) - C_\pi^2 H(x_2))\frac{\partial P^D}{\partial x_2}|_\Sigma + o(\frac{1}{\varepsilon}) + \text{ outer boundary layers,} \tag{16}$$

where $H(t)$ is the Heaviside function. We will see that $\mathcal{A}_\pi^k = C_\pi^2 \frac{\partial P^D}{\partial x_2}|_\Sigma$.

Next we follow references [1] and [24] and extend the pressure p^ε to Ω_2 by

$$\tilde{p}^\varepsilon(x) = \begin{cases} p^\varepsilon(x) & \text{for} \quad x \in \Omega^\varepsilon; \\ \dfrac{1}{\varepsilon^2|Y_F|}\displaystyle\int_{\varepsilon(Y_F-(k_1,k_2))} p^\varepsilon(y)\, dy & \text{in each } \varepsilon(Y_s - (k_1,k_2)). \end{cases} \tag{17}$$

$\mathbf{w}^i$, $i = 1, 2$ and $\beta^{2,bl}$ are extended by zero to the solid structure Y_S and $\mathbf{v}^\varepsilon$ by zero to $\Omega \setminus \Omega^\varepsilon$.

Theorem 1. *Let $\mathcal{O}$ be a neighborhood of $x_2 = -H$. Let us suppose the geometry and data smoothness as above and the compatibility condition (4). Let p^ε be extended to Ω_2 by formula (17).Then we have*

$$||\mathbf{v}^\varepsilon - \mathbf{u}^{eff}||_{L^2(\Omega_1)} \le C\sqrt{\varepsilon} \tag{18}$$
$$||\mathbf{v}^\varepsilon + \frac{\partial P^D}{\partial x_2}|_\Sigma (K_{22}\mathbf{e}^2 - \beta^{2,bl}(\frac{x_1}{\varepsilon}, 0+))||_{L^2(\Sigma)} \le C\sqrt{\varepsilon} \tag{19}$$
$$||\mathbf{v}^\varepsilon + \sum_{k=1}^{2}\frac{\partial P^D}{\partial x_k}\mathbf{w}^k(\frac{x}{\varepsilon}) - \frac{\partial P^D}{\partial x_2}|_\Sigma \beta^{2,bl}(\frac{x}{\varepsilon})||_{L^2(\Omega_2\setminus\mathcal{O})} \le C\varepsilon \tag{20}$$
$$||\tilde{p}^\varepsilon - H(-x_2)\varepsilon^{-2}P^D||_{L^2(\Omega)} \le \frac{C}{\varepsilon}. \tag{21}$$

Inspection of the proof of theorem (1) shows that we can obtain slightly better estimates by rearranging the term

$$\frac{1}{\varepsilon}(\omega^{2,bl}(\frac{x}{\varepsilon}) - C_\pi^2 H(x_2))\frac{\partial P^D}{\partial x_2}|_\Sigma.$$

We obtain

Theorem 2. *Let $\mathcal{O}$ be a neighborhood of $x_2 = -H$. Let us suppose the geometry and data smoothness as above and the compatibility condition (4). Let p^ε be extended to Ω_2 by formula (17).Then we have*

$$||\mathbf{v}^\varepsilon - \mathbf{u}^{eff} + C_1^{2,bl}\frac{\partial P^D}{\partial x_2}|_\Sigma \mathbf{e}^1 - \frac{\partial P^D}{\partial x_2}|_\Sigma \beta^{2,bl}(\frac{x}{\varepsilon})||_{L^2(\Omega_1)} \le C\varepsilon \tag{22}$$

$$||\mathbf{v}^\varepsilon + \frac{\partial P^D}{\partial x_2}|_\Sigma(\mathbf{w}^k(\frac{x_1}{\varepsilon}, 0-) - \beta^{2,bl}(\frac{x_1}{\varepsilon}, 0-))||_{L^2(\Sigma)} =$$

$$||\mathbf{v}^\varepsilon + \frac{\partial P^D}{\partial x_2}|_\Sigma(K_{22}\mathbf{e}^2 - \beta^{2,bl}(\frac{x_1}{\varepsilon}, 0+))||_{L^2(\Sigma)} \le C\varepsilon \tag{23}$$

$$||\mathbf{v}^\varepsilon + \sum_{k=1}^{2}\frac{\partial P^D}{\partial x_k}\mathbf{w}^k(\frac{x}{\varepsilon}) - \frac{\partial P^D}{\partial x_2}|_\Sigma \beta^{2,bl}(\frac{x}{\varepsilon})||_{L^2(\Omega_2\setminus\mathcal{O})} \le C\varepsilon \tag{24}$$

$$||\tilde{p}^\varepsilon - H(-x_2)(\varepsilon^{-2}P^D - \varepsilon^{-1}(C_\pi^2\frac{\partial P^D}{\partial x_2}|_\Sigma + \sum_{j=1}^{2}\tilde{\pi}^j(\frac{x}{\varepsilon})\frac{\partial P^D}{\partial x_j}))||_{L^2(\Omega)} \le \frac{C}{\sqrt{\varepsilon}}. \tag{25}$$

Remark 3. *We took as correction to P^D the quantity $-C_\pi^2\partial_{x_2}P^D|_\Sigma$. In fact the better choice would be to take a function satisfying equations (13a)-(13b), with value on Σ being $-C_\pi^2\partial_{x_2}P^D|_\Sigma$, instead of zero. Since the order of approximation does not change, we make the simplest possible choice.*

If the effective porous medium pressure is $P^{D,eff} = P^D - \varepsilon C_\pi^2\partial_{x_2}P^D|_\Sigma$, then the requirement that we can only have an $O(1)$ normal stress jump on Σ yields

$$P^{D,eff} + \varepsilon C_\pi^2\partial_{x_2}P^{D,eff} = O(\varepsilon^2) \quad on \quad \Sigma. \tag{26}$$

The relation (26) indicates presence of an effective pressure slip at the interface Σ. Since ε is related to the square root of the permeability, in the dimensional formulation, our result compares to the numerical experiments by Sahraoui and Kaviany in [20] and [31]. They found it being small for parallel flows. We find it small but of order of the corrections in the law by Beavers and Joseph in the case of the transverse flow.

Remark 4. *We obtain an expression for the tangential slip velocity. Since it is zero in the isotropic case, we do not confirm formulas like (86), page 2645, from [28] or like formula (31) for oblique flows from [31], which generalize the law by Beavers and Joseph.*

In [28], formula (71), page 2643, expresses the continuity of the averaged velocities. By construction, we have the trace continuity for our approximation. Nevertheless, one usually does not keep the boundary layers in the macroscopic model. If we eliminate the boundary layers and all low order terms, the effective velocity at the interface

Σ is

$$\mathbf{u}^{eff} = C_1^{2,bl}\frac{\partial P^D}{\partial x_2}\mathbf{e}^1 - K_{22}\frac{\partial P^D}{\partial x_2}\mathbf{e}^2,$$

(see (14d)) and from the porous media side

$$\mathbf{u}^D = -K_{12}\frac{\partial P^D}{\partial x_2}\mathbf{e}^1 - K_{22}\frac{\partial P^D}{\partial x_2}\mathbf{e}^2.$$

Therefore we find out that there is an effective tangential velocity jump at the interface.

3. Numerical confirmation of the effective interface conditions

This section is dedicated to the numerical confirmation of the analytical results shown above. We solve the problems needed to numerically compare the microscopic with the macroscopic problem by the finite element method (FEM). For the FEM theory we refer to standard literature, e.g., [8] or [5].

For the discretization of the Stokes system we use the Taylor-Hood element, which is inf-sup stable [6], therefore it does not need stabilization terms. In particular, since the homogenization error in some of the proposed estimates is small in comparison with the discretization error even for meshes with a number of elements in the order of millions, we have used higher order finite elements (polynomial of third degree for the velocity components and of second degree for the pressure) to reduce the discretization error.

The flow properties depend on the geometry of the pores. In particular there is a substantial difference between the case with symmetric inclusions with respect to the axis orthogonal to the interface and the case with asymmetric inclusions. We use therefore two different types of inclusion in the porous part, *circles* and rotated *ellipses*, i.e. ellipses with the major principal axis non parallel to the flow. The increased accuracy using higher order finite elements in the numerical solutions was necessary, as shown later, especially for the case with symmetric inclusions. The geometries of the unit cells $Y = (0.1)^2$, see Figure 3, for these two cases are as follows:

1. the solid part of the cell Y_s is formed by a circle with radius 0.25 and center $(0.5, 0.5)$.
2. Y_s consists of an ellipse with center $(0.5, 0.5)$ and semi-axes $a = 0.4$ and $b = 0.2$, which are rotated anti-clockwise by 45°.

In addition, since the considered domains have curved boundaries we use cells of the FEM mesh with curved boundaries (a mapping with polynomial of second degree was used for the geometry) to obtain a better approximation.

All computations are done using the toolkit `DOpElib` ([12]) based upon the C++-library `deal.II` ([2]).

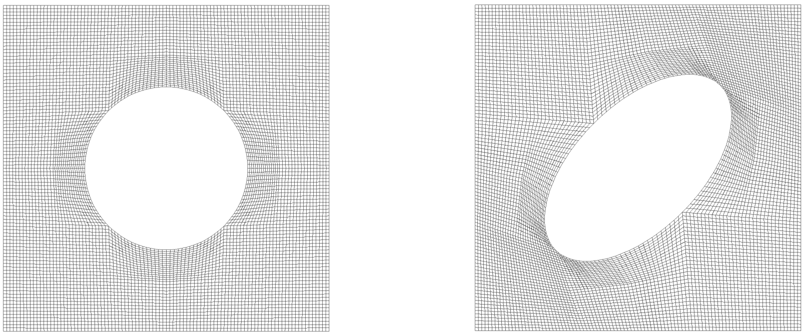

(a) Circle (b) Ellipse

Figure 3: Mesh of the fluid part of the unit cell for the two types of inclusions: circles and ellipses

3.1. Numerical setting

In this subsection we describe the setting for the numerical test. To confirm the estimates of Theorem 1 and 2 we have to solve the microscopic problem (3) to get $\mathbf{v}^{\varepsilon}$ and p^{ϵ}, the macroscopic problems (13) and (14) to get $\mathbf{u}^{eff}, p^{eff}$ and P^{D}, the cell problem (6) to calculate the permeability tensor K, the velocity vector $\mathbf{w}$ and pressure π, and the boundary layer (8) for the velocity $\boldsymbol{\beta}^{bl}$ and pressure ω^{bl}.

To reduce the discretization errors we consider a test case, described below, for which it is easy to derive the exact form of the macroscopic solution. As we will show below, the analytical solution of the macroscopic problem can be expressed in terms of the solution of the cell and boundary layer problems. The discretization error of the macroscopic problem in this case depends on the discretization error of the cell and boundary layer problems and does not imply therefore an additional discretization error.

We consider the following domains $\Omega = [0,1]\times[-1,1]$ and $\Omega^{\varepsilon} = \Omega\backslash$'the obstacles', where the obstacles are either circles or ellipses as described in the subsection above. In our example we consider the in- and outflow condition

$$\mathbf{v}^{D} = (0,-1) \text{ and } g = -1. \tag{27}$$

in the microscopic problem (3)

The macroscopic solution in this setting is

$$u_1^{\mathrm{eff}} = \frac{C_1^{2,bl}}{K_{22}}(1 - x_2), \tag{28a}$$

$$u_2^{\mathrm{eff}} = -1, \tag{28b}$$

$$p^{\mathrm{eff}} = 0, \tag{28c}$$

$$P^D = \frac{1}{K_{22}} x_2. \tag{28d}$$

The macroscopic solution depends on the solution of the cell problem though the permeability K, see expressions (28a) and (28d). Furthermore it depends on the solution of the boundary layer though the constant $C_1^{2,bl}$. The macroscopic problems (13) and (14) are therefore not numerically solved.

The microscopic problem (3) is solved with around 10–15 million degrees of freedom, the cell problem uses around 7 million degrees of freedom. The permeability constant has been precisely calculated using the goal oriented strategy for mesh adaptivity described in [7].

In the boundary layer problem, due to the interface condition (8c), the velocity as well as the pressure is discontinuous on the interface S. Since with the H^1 conform finite elements chosen for the discretization the discontinuity cannot be properly approximated, we have decided to transform the problem so that the solution variables are continuous across S. The values of $\boldsymbol{\beta}^{bl}$ and π^{bl} needed to check the estimates are recovered by post-processing. For the numerical solution, as explained in detail in the appendix of our previous work [7], we use a cut-off domain, which is justified by the exponential decaying of the boundary layer solution. The solution of the boundary layer problem is obtained with a mesh of around 4 million degrees of freedom and the constants $C_1^{2,bl}$ and C_π^{bl} are calculated by the goal oriented strategy for mesh adaptivity described in [7] where we have made sure that the cut-off error is smaller than the discretization error. We note that in the computation of C_π^2 we do not use the formula given in (12) but the equivalent one

$$\int_0^1 \omega^{j,bl}(y_1, 1)\, dy_1 \tag{29}$$

as this proved to be advantageous numerically.

In table 1 the computed constants $K, C_1^{2,bl}$ and C_π^{bl} for the two different inclusions are listed. As the permeability tensor K has for the given cases the form

$$K = \begin{pmatrix} K_{11} & K_{12} \\ K_{12} & K_{11} \end{pmatrix},$$

	circular inclusions	**oval inclusions**
K_{11}	0.0199014353519271 $\pm 2 \cdot 10^{-12}$	0.0122773324576884 $\pm 2 \cdot 10^{-13}$
K_{12}	0	0.00268891986291451 $\pm 2 \cdot 10^{-13}$
$C_1^{2,bl}$	0	-0.003336740001686 $\pm 4 \cdot 10^{-10}$
C_π^{bl}	0.025777570627281 $\pm 3 \cdot 10^{-8}$	-0.004429782196436 $\pm 1 \cdot 10^{-8}$

Table 1: Computed constants for the computations in the example.

i.e. it holds $K_{11} = K_{22}$ and $K_{12} = K_{21}$, we state only K_{11} and K_{12}. Additionally, we give an estimation of the discretization error.

3.2. Numerical results

In this section we present the numerical confirmation of the convergence rates of the homogenization errors (18–21) and (22–25).

For our test we set $\Omega_2 \setminus \mathcal{O} = [0,1] \times [-0.6, 0]$, and we use a computation of the boundary layer on a cut-off domain ranging from -4 to 4. This means that to compute the norms we evaluate the terms involving the boundary layer only for $x \in \Omega$ with $-4\epsilon < x_2 < 4\epsilon$. Outside of this region we assume the difference between the boundary layer components and their respective asymptotic values to be sufficiently small.

In the case of inclusions symmetric in the sense explained above, e.g. circles, the homogenization errors are much smaller than the numerical error even for large epsilon such as 0.1 as can be observed in Figure 4. The lines with markers represent the results of the computations for $\epsilon \in \{1, \frac{1}{3}, 0.1, \frac{1}{31}, 0.01\}$, the solid lines are reference values for various convergence rates and are plotted only to compare the respective slopes.

The case of circles is shown in Figure 4. For the velocity in the fluid part of the domain the estimate (18) can be verified. For the better estimate (22), that uses correction terms to improve the estimation, the homogenization error is so small that the curve shows only the numerical error, that in our case is only due to the discretization error since the quadrature error and the tolerance of the solver are smaller. In Figure 4b we can confirm (24) only for values of epsilon not bigger than $\frac{1}{31}$, for $\epsilon = 0.01$ the numerical error dominates the homogenization error. In the estimates for circles on the interface (Figure 4c) we can observe only the numerical error for the same reason explained above. Notice that the error for circles shown in Figure 4 is much smaller than the error for ellipses shown in Figure 5. In addition, we could verify both estimates for the pressure (21) and (25) as shown in Figure 4d. Note that the pressure estimates have been scaled multiplying by ϵ^2.

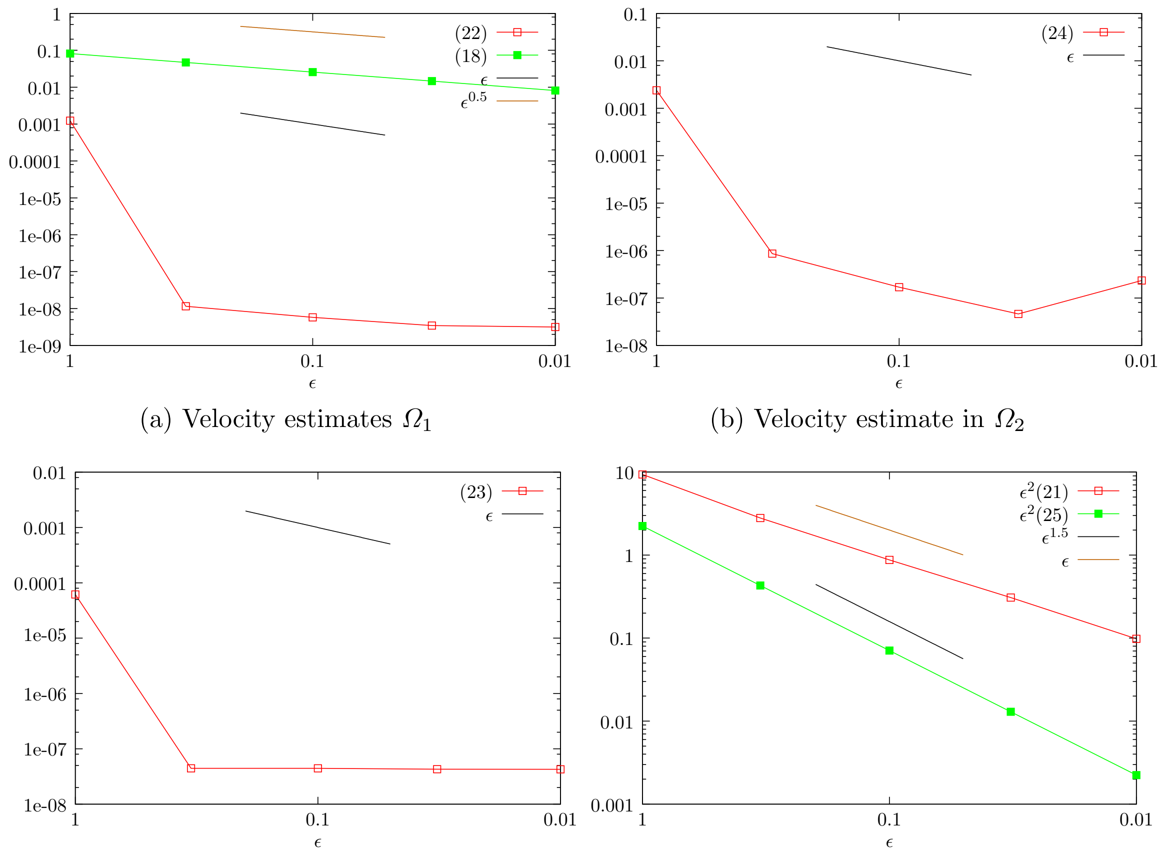

(a) Velocity estimates Ω_1

(b) Velocity estimate in Ω_2

(c) Velocity on Σ.

(d) Pressure estimates multiplied by ϵ^2

Figure 4: Convergence results for circles.

The case of ellipses is shown in Figure 5. As it can be observed, all estimates could be numerically verified, since the discretization error in this case was smaller than the homogenization error. Also in this case the pressure estimates have been scaled multiplied by ϵ^2. Note, that we observe for the velocity in the porous domain a convergence rate of 1.5 instead of the predicted first order convergence, see Figure 5b.

In conclusion, we show in Figure 6 and Figure 7 pictures of the flow for the case $\epsilon = \frac{1}{3}$. Since we use periodic boundary conditions in the x_1-direction, constant in- and outflow data as well as a periodic geometry, the computations have been performed on a stripe of one column of inclusions to reduce the computational effort. In Figure 6a and 6c we see streamline plots of the velocity, Figure 6b and 6d show the corresponding pressures. Both pressures are nearly constant in the fluid part and show then a linear descent to the outflow boundary, similar to the effective pressure

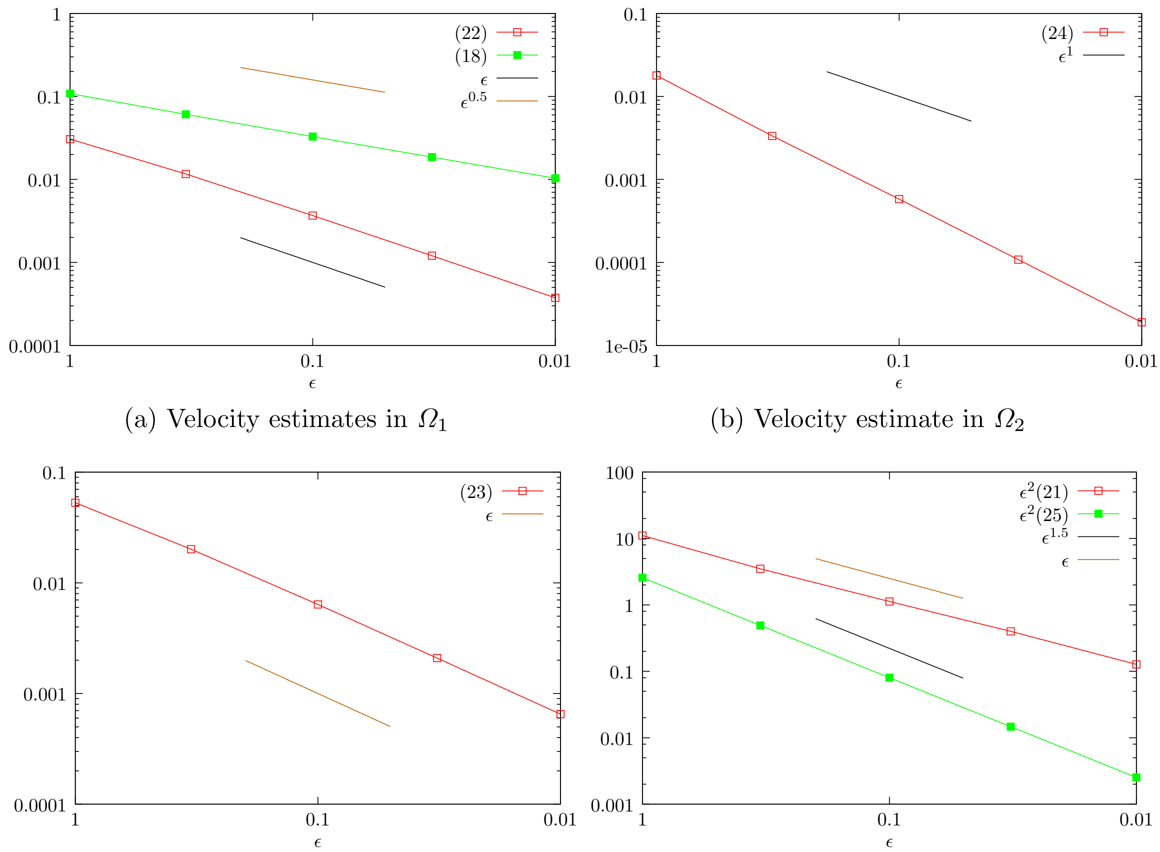

(a) Velocity estimates in Ω_1

(b) Velocity estimate in Ω_2

(c) Velocity components on Σ

(d) Pressure estimates multiplied by ϵ^2

Figure 5: Convergence results for elliptical inclusions.

(28c) and (28d).

Figure 7 shows only the values of the tangential velocity component. In the case of circular inclusions (figure 7a), the velocity is nearly zero throughout the fluid region and shows some oscillations around the mean value zero on the position of the interface. Note that the effective model prescribes here a no slip condition because it holds $C_1^{2,bl} = 0$. In Figure 7b) we see the corresponding solution for oval inclusions. We notice a linear descent from the inflow boundary (which lies in this picture on the left hand side) to the interface, which leads to the slip condition for the tangential velocity component of the effective flow in this case. Both behaviors are predicted from the effective interface condition for this velocity component, see (14d).

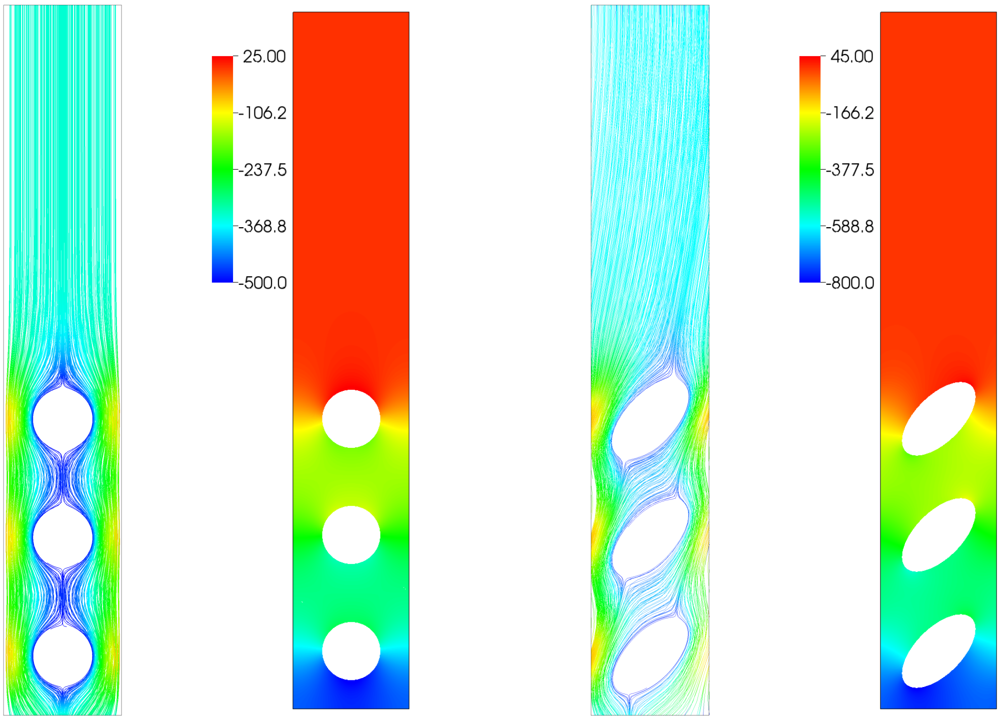

(a) Streamlines of $\mathbf{v}^\varepsilon$ (b) p^ϵ (c) Streamlines of $\mathbf{v}^\varepsilon$ (d) p^ϵ

Figure 6: Visualization of the solution to the microscopic problem for $\epsilon = \frac{1}{3}$. Subfigures (a)and (b) show the results for circular inclusions, (c)and (d) for elliptical inclusions.

4. Proof of Theorem 1 via incremental accuracy correction

In the proofs which follow we will frequently use the space

$$
\begin{aligned}
V_{per}(\Omega^\varepsilon) = \{\mathbf{z} \in H^1(\Omega^\varepsilon)^2 : \ \mathbf{z} = 0 \ \text{ on } \partial\Omega^\varepsilon \setminus \partial\Omega, \ \mathbf{z} = 0 \quad \text{on} \quad \{x_2 = h\}, \\
z_2 = 0 \quad \text{on} \quad \{x_2 = -H\} \quad \text{ and } \mathbf{z} \ \text{ is L-periodic in } x_1 \text{ variable } \}. \qquad (30)
\end{aligned}
$$

We will follow the strategy from [16], write a variational equation for the errors in velocity and in pressure and reduce the forcing term in several steps. We will frequently use the notation

$$
\mathbf{w}^{j,\varepsilon}(x) = \mathbf{w}^j(\frac{x}{\varepsilon}) \quad \text{and} \quad \pi^{j,\varepsilon}(x) = \pi^j(\frac{x}{\varepsilon}), \qquad (31)
$$

where $\{\mathbf{w}^j, \pi^j\}$ is given by (6).

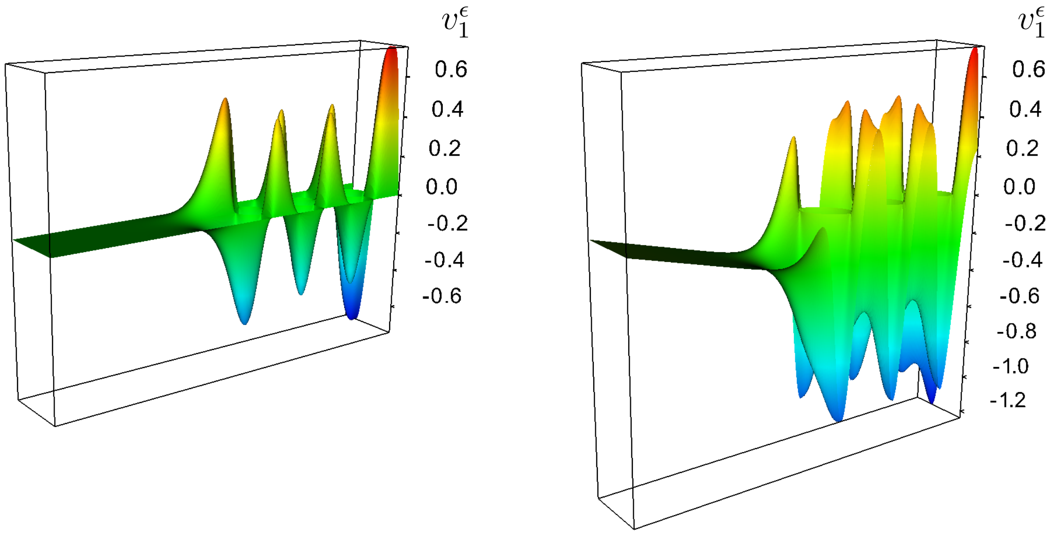

(a) Circular inclusions. (b) Elliptical inclusions.

Figure 7: Visualization of v_1^ϵ for $\epsilon = \frac{1}{3}$.

4.1. Incremental accuracy correction, the 1st part

Proposition 5. *Let P^D given by (13a)-(13b), $\{\mathbf{u}^{eff}, p^{eff}\}$ be the solution for (14a)-(14d) and $\{\mathbf{w}^{j,\varepsilon}, \pi^{j,\varepsilon}\}$ defined by (31). Let $\{\mathbf{v}^\varepsilon, p^\varepsilon\}$ be the solution for (3a)-(3d). Then for every $\varphi \in V_{per}(\Omega^\varepsilon)$ we have*

$$|\langle \mathcal{L}^\varepsilon, \varphi\rangle| = |\int_{\Omega^\varepsilon} \{\nabla \mathbf{v}^\varepsilon - H(x_2)\nabla \mathbf{u}^{eff} +$$

$$H(-x_2)\nabla \sum_{j=1}^{2} \mathbf{w}^{j,\varepsilon} \frac{\partial P^D}{\partial x_j}\}\nabla\varphi \; dx - \int_{\Omega^\varepsilon} \{p^\varepsilon - H(x_2)p^{eff} -$$

$$H(-x_2)(\varepsilon^{-2}P^D - \varepsilon^{-1}\sum_{j=1}^{2} \pi^{j,\varepsilon}\frac{\partial P^D}{\partial x_j})\} \;\; div\, \varphi \; dx + \int_{\{x_2=-H\}} \sum_{j=1}^{2} \frac{\partial}{\partial x_2}(w_1^{j,\varepsilon}\frac{\partial P^D}{\partial x_j})\varphi_1 \; dS$$

$$-\int_{\Sigma} \Big(\sigma_0\varphi + \sum_{j=1}^{2}(\nabla \mathbf{w}^{j,\varepsilon} - \varepsilon^{-1}\pi^{j,\varepsilon} I)\frac{\partial P^D}{\partial x_j}\mathbf{e}^2\varphi\Big) \; dS| \le C\|\nabla\varphi\|_{L^2(\Omega_2^\varepsilon)^4}, \qquad (32)$$

where $\sigma_0 = (\nabla \mathbf{u}^{eff} - p^{eff} I)\mathbf{e}^2$ on Σ.

Proof of proposition 5 We start with the weak formulation corresponding to (3a)-(3d):

$$\int_{\Omega^\varepsilon} \nabla \mathbf{v}^\varepsilon \nabla \varphi - \int_{\Omega^\varepsilon} p^\varepsilon \ \operatorname{div} \varphi = 0, \quad \forall \varphi \in V_{per}(\Omega^\varepsilon). \tag{33}$$

As a first step we eliminate the boundary conditions. The weak formulation corresponding to system (14a)-(14d) is

$$\int_{\Omega_1} \nabla \mathbf{u}^{eff} \nabla \varphi - \int_{\Omega_1} p^{eff} \ \operatorname{div} \varphi = - \int_{\Sigma} \sigma_0 \varphi \ dS, \quad \forall \varphi \in V_{per}(\Omega^\varepsilon). \tag{34}$$

Next the weak formulation corresponding to the correction in the pore space Ω_2^ε is

$$\begin{aligned} &\int_{\Omega_2^\varepsilon} (-\nabla \sum_{j=1}^{2} \mathbf{w}^{j,\varepsilon} \frac{\partial P^D}{\partial x_j} - \varepsilon^{-2} P^D I + \varepsilon^{-1} \sum_{j=1}^{2} \pi^{j,\varepsilon} \frac{\partial P^D}{\partial x_j} I) \nabla \varphi \ dx = \int_{\Omega_2^\varepsilon} (\mathbf{w}^{j,\varepsilon} \Delta \frac{\partial P^D}{\partial x_j} + \\ &2 \nabla \mathbf{w}^{j,\varepsilon} \nabla \frac{\partial P^D}{\partial x_j} - \varepsilon^{-1} \pi^{j,\varepsilon} \nabla \frac{\partial P^D}{\partial x_j}) \cdot \varphi \ dx - \int_{\Sigma} \sum_{j=1}^{2} \Big\{ (\nabla \mathbf{w}^{j,\varepsilon} - \varepsilon^{-1} \pi^{j,\varepsilon} I) \frac{\partial P^D}{\partial x_j} \mathbf{e}^2 + \\ &\frac{\partial^2 P^D}{\partial x_2 \partial x_j} \mathbf{w}^{j,\varepsilon} \Big\} \cdot \varphi \ dS + \int_{\{x_2 = -H\}} \sum_{j=1}^{2} \frac{\partial}{\partial x_2} (w_1^{j,\varepsilon} \frac{\partial P^D}{\partial x_j}) \varphi_1 \ dS, \quad \forall \varphi \in V_{per}(\Omega^\varepsilon). \end{aligned} \tag{35}$$

We observe that difference between (33) and (34)-(35) is equivalent to

$$\langle \mathcal{L}^\varepsilon, \varphi \rangle = \int_{\Omega_2^\varepsilon} \varphi \sum_{j=1}^{2} A_\varepsilon^j + \int_{\Sigma} \sum_{j=1}^{2} \mathbf{w}^{j,\varepsilon} \frac{\partial^2 P^D}{\partial x_2 \partial x_j} \cdot \varphi \ dS, \tag{36}$$

where quantities A_ε^j are given by

$$\begin{aligned} A_\varepsilon^j &= -\mathbf{w}^{j,\varepsilon} \Delta \frac{\partial P^D}{\partial x_j} - 2 \nabla \mathbf{w}^{j,\varepsilon} \nabla \frac{\partial P^D}{\partial x_j} + \varepsilon^{-1} \pi^{j,\varepsilon} \nabla \frac{\partial P^D}{\partial x_j} = \\ &\mathbf{w}^{j,\varepsilon} \Delta \frac{\partial P^D}{\partial x_j} + \varepsilon^{-1} \pi^{j,\varepsilon} \nabla \frac{\partial P^D}{\partial x_j} - 2 \ \operatorname{div} \ \{ \nabla \frac{\partial P^D}{\partial x_j} \otimes \mathbf{w}^{j,\varepsilon} \}, \ j = 1, 2. \end{aligned} \tag{37}$$

We note that

$$-\nabla \sum_{j=1}^{2} \mathbf{w}^j (\frac{x}{\varepsilon}) \frac{\partial P^D}{\partial x_j} = - \sum_{j=1}^{2} \nabla \mathbf{w}^j (\frac{x}{\varepsilon}) \frac{\partial P^D}{\partial x_j} - \sum_{j=1}^{2} \nabla \frac{\partial P^D}{\partial x_j} \otimes \mathbf{w}^{j,\varepsilon}.$$

and a straightforward calculation yields

$$|\int_{\Omega_2^\varepsilon} \varphi \sum_j A_\varepsilon^j| \leq C\|\nabla\varphi\|_{L^2(\Omega_2^\varepsilon)^4} \tag{38}$$

$$|\int_\Sigma \sum_{j=1}^2 \mathbf{w}^j(\frac{x}{\varepsilon})\frac{\partial^2 P^D}{\partial x_2 \partial x_j} \cdot \varphi \; dS| \leq C\sqrt{\varepsilon}\|\nabla\varphi\|_{L^2(\Omega_2^\varepsilon)^4}. \tag{39}$$

∎

Remark 6. *Now we see why it is necessary to impose $P^D = 0$ at the interface Σ. Without it there would be a term $\int_\Sigma \varepsilon^{-2} P^D \varphi_2 \; dS$ at the right hand side of (35).*

Remark 7. *The candidate for the approximation of $\{\mathbf{v}^\varepsilon, p^\varepsilon\}$ is*

$$\begin{cases} \mathbf{v}^\varepsilon \approx H(x_2)\mathbf{u}^{eff} - H(-x_2)\sum_{j=1}^2 \mathbf{w}^{j,\varepsilon}\dfrac{\partial P^D}{\partial x_j}; \\ p^\varepsilon \approx H(x_2)p^{eff} + H(-x_2)(\varepsilon^{-2}P^D - \varepsilon^{-1}\sum_{j=1}^2 \pi^{j,\varepsilon}\dfrac{\partial P^D}{\partial x_j}). \end{cases} \tag{40}$$

Unfortunately, with such approximation we do not have continuity of the trace of the velocity approximation on the interface Σ.

4.2. Incremental accuracy correction, the 2nd part

The idea is to insert the correction to $\mathbf{v}^\varepsilon$ as the test function φ in equation (36). Therefore the correction should be an element of $V_{per}(\Omega^\varepsilon)$ and in this step we eliminate the trace jump on Σ. As in [16], fixing the traces on Σ requires using the boundary layers defined by (8a)-(8e). At this stage we introduce the error functions

$$\begin{aligned} \mathbf{U}^\varepsilon = \mathbf{v}^\varepsilon - H(x_2)(\mathbf{u}^{eff} - \mathbf{e}^1 C_1^{2,bl}\frac{\partial P^D}{\partial x_2}|_\Sigma) + \\ H(-x_2)\sum_{j=1}^2 \mathbf{w}^{j,\varepsilon}\frac{\partial P^D}{\partial x_j} - \beta^{2,bl,\varepsilon}\frac{\partial P^D}{\partial x_2}|_\Sigma; \end{aligned} \tag{41}$$

$$\begin{aligned} P^\varepsilon = p^\varepsilon - H(x_2)p^{eff} - H(-x_2)(\varepsilon^{-2}P^D - \varepsilon^{-1}\sum_{j=1}^2 \pi^{j,\varepsilon}\frac{\partial P^D}{\partial x_j}) \\ -\varepsilon^{-1}(\omega^{2,bl,\varepsilon} - C_\pi^2)\frac{\partial P^D}{\partial x_2}|_\Sigma, \end{aligned} \tag{42}$$

where $\{\beta^{2,bl,\varepsilon}, \omega^{2,bl,\varepsilon}\}(x) = \{\beta^{2,bl}, \omega^{2,bl}\}(\frac{x}{\varepsilon})$ are defined by (8a)-(8e) and $(C^{2,bl}, C_\pi^2)$ by (9).

Proposition 8. $\mathbf{U}^\varepsilon \in H^1(\Omega^\varepsilon)^2$ *and for all* $\varphi \in V_{per}(\Omega^\varepsilon)$ *we have*

$$|\int_{\Omega^\varepsilon} \nabla \mathbf{U}^\varepsilon \nabla \varphi \, dx - \int_{\Omega^\varepsilon} P^\varepsilon \; div \, \varphi \, dx + \int_{\{x_2=-H\}} \sum_{j=1}^{2} \frac{\partial}{\partial x_2} (w_1^{j,\varepsilon} \frac{\partial P^D}{\partial x_j}) \varphi_1 \, dS| \leq$$
$$C \|\nabla \varphi\|_{L^2(\Omega_2^\varepsilon)^4} + \|\varphi\|_{H^1(\Omega_1)^2}. \tag{43}$$

Proof of proposition 8 . We have the following variational equation for $\{\mathbf{U}^\varepsilon, P^\varepsilon\}$, for all $\varphi \in V_{per}(\Omega^\varepsilon)$,:

$$\int_{\Omega^\varepsilon} \nabla \mathbf{U}^\varepsilon \nabla \varphi \, dx - \int_{\Omega^\varepsilon} P^\varepsilon \; \text{div} \, \varphi \, dx = \int_\Sigma (\sigma_0 + \sum_{j=1}^2 B_\varepsilon^j) \mathbf{e}^2 \varphi \, dS -$$
$$\int_{\{x_2=-H\}} \mathcal{C}_\varepsilon^1 \varphi_1 \, dS + \int_{\Omega_2^\varepsilon} \varphi (\sum_{j=1}^2 A_\varepsilon^j - A_\varepsilon^{22}) \, dx - 2 \int_{\Omega^\varepsilon} A_\varepsilon^{12} \nabla \varphi \, dx$$
$$- \int_{\Omega_1} (A_\varepsilon^{32} + A_\varepsilon^{42}) \varphi \, dx, \tag{44}$$

where

$$B^j = -\mathbf{w}^{j,\varepsilon} \otimes \nabla \frac{\partial P^D}{\partial x_j}, \tag{45}$$

$$A_\varepsilon^{12} = -\frac{d}{dx_1} (\frac{\partial P^D}{\partial x_2} |_\Sigma) \mathbf{e}^1 \otimes (\beta^{2,bl,\varepsilon} - H(x_2) C^{2,bl}), \tag{46}$$

$$A_\varepsilon^{22} = -\beta^{2,bl,\varepsilon} \frac{d^2}{dx_1^2} (\frac{\partial P^D}{\partial x_2} |_\Sigma) - \varepsilon^{-1} (\omega^{2,bl,\varepsilon} - C_\pi^2) \frac{d}{dx_1} (\frac{\partial P^D}{\partial x_2} |_\Sigma) \mathbf{e}^1, \tag{47}$$

$$A_\varepsilon^{32} = -(\beta^{2,bl,\varepsilon} - C_1^{2,bl} \mathbf{e}^1) \frac{d^2}{dx_1^2} (\frac{\partial P^D}{\partial x_2} |_\Sigma), \tag{48}$$

$$A_\varepsilon^{42} = -\varepsilon^{-1} (\omega^{2,bl,\varepsilon} - C_\pi^2) \frac{d}{dx_1} (\frac{\partial P^D}{\partial x_2} |_\Sigma) \mathbf{e}^1, \tag{49}$$

$$\mathcal{C}_\varepsilon^1 = \frac{\partial U_1^\varepsilon}{\partial x_2} |_{\{x_2=-H\}} = \sum_{j=1}^2 \frac{\partial}{\partial x_2} (w_1^{j,\varepsilon} \frac{\partial P^D}{\partial x_j}) |_{\{x_2=-H\}} + \text{exponentially small terms.} \tag{50}$$

Then we have

$$|\int_\Sigma \sum_{j=1}^2 B^j \mathbf{e}^2 \varphi \, |\leq C \varepsilon^{1/2} \|\nabla \varphi\|_{L^2(\Omega_2^\varepsilon)^4}. \tag{51}$$

Now we turn to the volume terms. We have

$$| \int_{\Omega^\varepsilon} \sum_j A_\varepsilon^{12} \nabla\varphi \, dx | \leq C\varepsilon^{1/2} \|\nabla\varphi\|_{L^2(\Omega^\varepsilon)^4} \tag{52}$$

$$| \int_{\Omega_2^\varepsilon} \sum_j A_\varepsilon^{22} \varphi \, dx | \leq C \|\nabla\varphi\|_{L^2(\Omega_2^\varepsilon)^4} \tag{53}$$

$$| \int_{\Omega_1} \sum_j A_\varepsilon^{32} \varphi \, dx | \leq C\sqrt{\varepsilon} \|\varphi\|_{L^2(\Omega_1)^2}. \tag{54}$$

Finally, we estimate the term involving A_ε^{42}. Let Q^2 be defined by

$$\begin{cases} \dfrac{\partial Q^2}{\partial y_1} = \omega^{2,bl} - C_\pi^2, & \text{on } (0,1) \times (0,+\infty); \\ Q^2 & \text{is } y_1 - \text{periodic.} \end{cases} \tag{55}$$

By definition of C_π^2, the function

$$Q^2(y_1,y_2) = \int_0^{y_1} \omega^{2,bl}(t,y_2) dt - C_\pi^2 y_1, \quad y \in (0,1) \times (0,+\infty) \tag{56}$$

is a solution for (55) and, using the results from [16], page 459, there exists a constant $\gamma_0 > 0$ such that $e^{\gamma_0 y_2} Q^j \in L^2(Z^+)$.

We set $Q^{2,\varepsilon}(x) = \varepsilon Q^2(x/\varepsilon)$, $x \in \Omega_1$. Then we obtain

$$\begin{cases} \dfrac{\partial Q^{2,\varepsilon}}{\partial x_1} = \omega^{2,bl,\varepsilon}(x) - C_\pi^2; \\ \|Q^{2,\varepsilon}\|_{L^2(\Omega_1)} \leq C\varepsilon^{3/2}. \end{cases} \tag{57}$$

Therefore we have

$$\begin{aligned} | \int_{\Omega_1} A_\varepsilon^{42} \varphi \, dx | &= | \int_{\Omega_1} \varepsilon^{-1} Q^{2,\varepsilon} (\varphi_1 \frac{d^2}{dx_1^2} (\frac{\partial P^D}{\partial x_2}|_\Sigma) + \frac{\partial \varphi_1}{\partial x_1} \frac{\partial}{\partial x_1} (\frac{\partial P^D}{\partial x_2}|_\Sigma)) | \\ &\leq C\varepsilon^{1/2} \|\varphi\|_{H^1(\Omega_1)^2}. \end{aligned} \tag{58}$$

Now the estimates (51) - (58) show that the right hand side in (44) is bounded by

$$C\|\nabla\varphi\|_{L^2(\Omega_2^\varepsilon)^4} + C\varepsilon^{1/2} \|\varphi\|_{H^1(\Omega_1)^2}.$$

∎

Remark 9. *We would like to use* $\mathbf{U}^\varepsilon$ *as a test function in the variational equation (44). The difficulty with* $\mathbf{U}^\varepsilon$ *is that the boundary condition at* $\{x_2 = -H\}$ *is not satisfied. Hence we have to adjust its values at that boundary.*

4.3. Incremental accuracy correction, the 3rd part: correction of the outer boundary effects

First we calculate values of U_2^ε and $\dfrac{\partial}{\partial x_2}U_1^\varepsilon$ at the lower outer boundary $\{x_2 = -H\}$. We have

$$U_2^\varepsilon(x_1,-H) = v_2^\varepsilon(x_1,-H) + \sum_{j=1}^2 \frac{\partial P^D}{\partial x_j}(x_1,-H)K_{2j} + \sum_{j=1}^2 \frac{\partial P^D}{\partial x_j}(x_1,-H)(w_2^j(\frac{x_1}{\varepsilon},0) - K_{2j})$$

$$+O(e^{Cx_2/\varepsilon}) = \sum_{j=1}^2 \frac{\partial P^D}{\partial x_j}(x_1,-H)(w_2^j(\frac{x_1}{\varepsilon},0) - K_{2j}) + \text{ exponentially small terms},$$

$$\frac{\partial}{\partial x_2}U_1^\varepsilon(x_1,-H) = \frac{1}{\varepsilon}\sum_{j=1}^2 \frac{\partial P^D}{\partial x_j}(x_1,-H)\frac{\partial w_1^j}{\partial y_2}(\frac{x_1}{\varepsilon},0) + \sum_{j=1}^2 \frac{\partial^2 P^D}{\partial x_j \partial x_2}(x_1,-H)w_1^j(\frac{x_1}{\varepsilon},0)$$

$$+ \text{exponentially small terms.}$$

We follow again [16] and correct the outer boundary effects using the corresponding boundary layer:

$$-\triangle \mathbf{q}^{j,bl} + \nabla z^{j,bl} = 0 \qquad \text{in } Z^- \tag{59}$$

$$\text{div } \mathbf{q}^{j,bl} = 0 \qquad \text{in } Z^- \tag{60}$$

$$q_2^{j,bl} = K_{2j} - w_2^j \quad \text{and} \quad \frac{\partial q_1^j}{\partial y_2} = -\frac{\partial w_1^j}{\partial y_2} \text{ on } S \tag{61}$$

$$\mathbf{q}^{j,bl} = 0 \quad \text{ on } \cup_{k=1}^\infty \{\partial Y_F \setminus \partial Y - (0,k)\}, \quad \{\mathbf{q}^{j,bl}, z^{j,bl}\} \text{ is } y_1-\text{periodic}. \tag{62}$$

Following the theory from [16], problem (59)-(62) admits a unique solution $\mathbf{q}^{j,bl} \in H^1(Z^-)^2$, smooth in Z^-. Furthermore, there is $\gamma_0 > 0$ such that $e^{\gamma_0|y_2|}\mathbf{q}^{j,bl} \in L^2(Z^-)^2$ and, after adjusting a constant, $e^{\gamma_0|y_2|}z^{j,bl} \in L^2(Z^-)$. The new error functions read

$$\mathbf{U}^{1,\varepsilon} = \mathbf{U}^\varepsilon + \sum_{j=1}^2 \frac{\partial P^D}{\partial x_j}(x_1,-H)\mathbf{q}^{j,bl}(\frac{x_1}{\varepsilon}, -\frac{x_2+H}{\varepsilon}), \tag{63}$$

$$P^{1,\varepsilon} = P^\varepsilon + \frac{1}{\varepsilon}\sum_{j=1}^2 \frac{\partial P^D}{\partial x_j}(x_1,-H)z^{j,bl}(\frac{x_1}{\varepsilon}, -\frac{x_2+H}{\varepsilon}). \tag{64}$$

Variational equation (44) becomes

$$
\begin{aligned}
&\int_{\Omega^\varepsilon} \nabla \mathbf{U}^{1,\varepsilon} \nabla \varphi \, dx - \int_{\Omega^\varepsilon} P^{1,\varepsilon} \ \text{div } \varphi \, dx = \int_\Sigma \big(\sigma_0 + \sum_{j=1}^2 B_\varepsilon^j\big) \mathbf{e}^2 \varphi \, dS - \\
&\int_{\{x_2=-H\}} \sum_{j=1}^2 w_1^{j,\varepsilon} \varphi_1 \frac{\partial^2 P^D}{\partial x_j \partial x_2} \, dS + \int_{\Omega_2^\varepsilon} \varphi \big(\sum_{j=1}^2 A_\varepsilon^j - A_\varepsilon^{22}\big) \, dx - 2 \int_{\Omega^\varepsilon} A_\varepsilon^{12} \nabla \varphi \, dx \\
&- \int_{\Omega_1} (A_\varepsilon^{32} + A_\varepsilon^{42}) \varphi \, dx - 2 \int_{\Omega_2^\varepsilon} \sum_{j=1}^2 \nabla \mathbf{q}^{j,bl} \big(\frac{x_1}{\varepsilon}, -\frac{x_2+H}{\varepsilon}\big) \nabla \frac{\partial P^D}{\partial x_j}(x_1, -H) \varphi \, dx - \\
&\int_{\Omega_2^\varepsilon} \sum_{j=1}^2 \big(\Delta \frac{\partial P^D}{\partial x_j}(x_1, -H) \mathbf{q}^{j,bl}\big(\frac{x_1}{\varepsilon}, -\frac{x_2+H}{\varepsilon}\big) + \\
&\frac{1}{\varepsilon} \nabla \frac{\partial P^D}{\partial x_j}(x_1, -H) z^{j,bl}\big(\frac{x_1}{\varepsilon}, -\frac{x_2+H}{\varepsilon}\big)\big) \varphi \, dx.
\end{aligned}
\tag{65}
$$

The form of the right hand side of variational equation (65) yields

Proposition 10. *We have* $\mathbf{U}^{1,\varepsilon} \in V_{per}(\Omega^\varepsilon)$ *and* $\forall \varphi \in V_{per}(\Omega^\varepsilon)$ *we have*

$$
\Big| \int_{\Omega^\varepsilon} \nabla \mathbf{U}^{1,\varepsilon} \nabla \varphi \, dx - \int_{\Omega^\varepsilon} P^{1,\varepsilon} \ div \ \varphi \, dx \Big| \leq C \big(\|\nabla \varphi\|_{L^2(\Omega_2^\varepsilon)^4} + \|\varphi\|_{H^1(\Omega_1)^2} \big). \tag{66}
$$

Remark 11. *It remains to estimate the pressure through the velocity and then to use the velocity error as a test function in equation (44). However at this stage the difficulties are coming from the compressibility effects in the term* $\int_{\Omega^\varepsilon} P^\varepsilon \ div \ \mathbf{U}^\varepsilon \, dx$. *In fact*

$$
\begin{aligned}
div \ \mathbf{U}^{1,\varepsilon} = H(-x_2) \sum_{j=1}^2 \mathbf{w}^{j,\varepsilon} \nabla \frac{\partial P^D}{\partial x_j} + (\beta_1^{2,bl,\varepsilon} - H(x_2) C_1^{2,bl}) \frac{d}{dx_1} \big(\frac{\partial P^D}{\partial x_2}|_\Sigma \big) \\
+ \sum_{j=1}^2 \frac{d}{dx_1} \frac{\partial P^D}{\partial x_j}(x_1, -H) q_1^{j,bl}\big(\frac{x_1}{\varepsilon}, -\frac{x_2+H}{\varepsilon}\big)
\end{aligned}
$$

and the estimate of the divergence is $\| \ div \ \mathbf{U}^{1,\varepsilon}\|_{L^2(\Omega^\varepsilon)} \leq C$. *To solve the problem, we need to obtain the estimate of order epsilon for* $div \ \mathbf{U}^{1,\varepsilon}$ *in* $L^2(\Omega^\varepsilon)$.

4.4. Incremental accuracy correction, the 4th step: correction of the compressibility effects

We start by introducing the compressibility effects correction:

$$\begin{cases} \operatorname{div}_y \gamma^{j,i} = w_i^j - \dfrac{K_{ij}}{\mid Y_F \mid} \quad \text{in} \quad Y_F; \\ \gamma^{j,i} = 0 \quad \text{on } \partial Y_F \setminus \partial Y, \quad \gamma^{j,i} \quad \text{is} \quad 1-\text{periodic}. \end{cases} \tag{67}$$

The existence of at least one $\gamma^{j,i} \in H^1(Y_F)^2 \cap C^\infty_{loc}\big(\cup_{k\in\mathbb{N}}(Y_F-(0,k))^2\big)$, satisfying (67) is straightforward.

We introduce $\gamma^{j,i,\varepsilon}$ by

$$\gamma^{j,i,\varepsilon}(x) = \varepsilon \gamma^{j,i}(x/\varepsilon), \quad x \in \Omega_2^\varepsilon \tag{68}$$

and extend it by zero to $\Omega_2 \setminus \Omega_2^\varepsilon$.

$\gamma^{j,i,\varepsilon}$ is defined only in the porous part Ω_2 and an auxiliary boundary layer velocity and pressures, correcting its values of on Σ, is needed.

First we construct $\{\gamma^{j,i,bl}, \pi^{j,i,bl}\}$ satisfying

$$-\triangle_y \gamma^{j,i,bl} + \nabla_y \pi^{j,i,bl} = 0 \qquad \text{in } Z^+ \cup Z^-, \tag{69}$$

$$\operatorname{div}_y \gamma^{j,i,bl} = 0 \qquad \text{in } Z^+ \cup Z^-, \tag{70}$$

$$\big[\gamma^{j,i,bl}\big]_S(\cdot,0) = \gamma^{j,i}(\cdot,0) \quad \text{on } S, \tag{71}$$

$$\big[\{\nabla_y \gamma^{j,i,bl} - \pi^{j,i,bl} I\}\mathbf{e}^2\big]_S(\cdot,0) = \nabla_y \gamma^{j,i}(\cdot,0)\mathbf{e}^2 \ \text{ on } S, \tag{72}$$

$$\gamma^{j,i,bl} = 0 \quad \text{on } \cup_{k=1}^\infty \{\partial Y_F \setminus \partial Y - (0,k)\}, \quad \{\gamma^{j,i,bl}, \pi^{j,i,bl}\} \text{ is } y_1-\text{periodic}. \tag{73}$$

Proposition 3.19 from [16] gives the existence of a solution $\{\gamma^{j,i,bl}, \pi^{j,i,bl}\} \in V \cap C^\infty_{\text{loc}}(Z^+\cup Z^-)^2 \times C^\infty_{\text{loc}}(Z^+\cup Z^-)$ to equations (69)-(73), where $\gamma^{j,i,bl}$ is uniquely determined and $\pi^{j,i,bl}$ is unique up to a constant. $\gamma^{j,i,bl}(\cdot,\pm 0) \in W^{2-1/q,q}(S)^2$ and $\{\nabla\gamma^{j,i,bl} - \pi^{j,i,bl} I\}(\cdot,\pm 0)e_2 \in W^{1-1/q,q}(S)^2$, $\forall q \in [1,\infty[$, but the limits from two sides of S are in general different. Furthermore, it is proved that there exist constants $\gamma_0 \in]0,1[, C_\pi^{j,i}$, and a constant vector $C^{j,i,bl}$ such that

$$e^{\gamma_0|y_2|}\nabla_y \gamma^{j,i,bl} \in L^2(Z^+\cup Z^-)^4,\ e^{\gamma_0|y_2|}\gamma^{j,i,bl} \in L^2(Z^-)^2, e^{\gamma_0|y_2|}(\pi^{j,i,bl} - C_\pi^{j,i}) \in L^2(Z^+)$$

and

$$\begin{cases} \mid \gamma^{j,i,bl}(y_1,y_2) - \mathbf{C}^{j,i,bl} \mid \leq Ce^{-\gamma_0 y_2}, \qquad y_2 > y_*; \\ \mid \pi^{j,i,bl}(y_1,y_2) - C_\pi^{j,i} \mid \leq Ce^{-\gamma_0 y_2}, \qquad y_2 > y_*. \end{cases} \tag{74}$$

We define

$$\gamma^{j,i,bl,\varepsilon}(x) = \varepsilon\gamma^{j,i,bl}(\frac{x}{\varepsilon}) \qquad \text{and} \qquad \pi^{j,i,bl,\varepsilon}(x) = \pi^{j,i,bl}(\frac{x}{\varepsilon}), \quad x \in \Omega^\varepsilon, \tag{75}$$

and extend $\gamma^{j,i,bl,\varepsilon}$ by zero to $\Omega \setminus \Omega^\varepsilon$.

Next, we need a correction for the compressibility effects coming from the boundary layer term $\beta^{2,bl,\varepsilon}\dfrac{\partial P^D}{\partial x_2}|_\Sigma$: We look for θ^{bl} satisfying

$$\begin{cases} \text{div } \theta^{bl} = \beta_1^{2,bl} - C_1^{2,bl} H(y_2) \quad \text{in } Z^+ \cup Z^-; \\ \left[\theta^{bl}\right]_S = (\displaystyle\int_{Z_{BL}} (C_1^{2,bl} H(y_2) - \beta_1^{2,bl})\ dy)\mathbf{e}^2 \quad \text{on } S; \\ \theta^{bl} = 0 \quad \text{on } \cup_{k=1}^\infty \{\partial Y_F \setminus \partial Y - (0,k)\}, \quad \theta^{bl} \quad \text{is } y_1 - \text{periodic.} \end{cases} \tag{76}$$

After proposition 3.20 from [16], problem (76) has at least one solution $\theta^{bl} \in H^1(Z^+ \cup Z^-)^2 \cap C^\infty_{loc}(Z^+ \cup Z^-)^2$. Furthermore, $\theta^{bl} \in W^{1,q}((0,1)^2)^2$ and $\theta^{bl} \in W^{1,q}(Y-(0,1))^2$, $\forall q \in [1,\infty)$ and there is $\gamma_0 > 0$ such that $e^{\gamma_0|y_2|}\theta^{j,i,bl} \in H^1(Z^+ \cup Z^-)^2$.

Let $\gamma^{j,i,\varepsilon}$ be defined by (68) and $\gamma^{j,i,bl,\varepsilon}, \pi^{j,i,bl,\varepsilon}, C_\pi^{j,i}, \mathbf{C}^{j,i,bl}$ by (74)-(75). We modify $\{\mathbf{u}^{eff}, p^{eff}\}$ by adding to it $\varepsilon\{\mathbf{u}^{1,eff}, p^{1,eff}\}$, satisfying (14a)-(14c) and with (14d) replaced by

$$u_2^{1,eff} = -\sum_{j,k=1}^{2} C_2^{j,k,bl} \frac{\partial^2 P^D}{\partial x_j \partial x_k}|_\Sigma - \theta_2^{bl}(\frac{x}{\varepsilon})\frac{d}{dx_1}\frac{\partial P^D}{\partial x_2}|_\Sigma \quad \text{on} \quad \Sigma, \tag{77}$$

$$u_1^{1,eff} = -\sum_{j,k=1}^{2} C_1^{j,k,bl} \frac{\partial^2 P^D}{\partial x_j \partial x_k}|_\Sigma - \theta_1^{bl}(\frac{x}{\varepsilon})\frac{d}{dx_1}\frac{\partial P^D}{\partial x_2}|_\Sigma \quad \text{on} \quad \Sigma. \tag{78}$$

The pair $\{\mathbf{u}^{1,eff}, p^{1,eff}\}$ is uniquely defined by (14a)-(14c), (77)-(78).

Finally we correct the compressibility effects coming from the boundary layer around $\{x_2 = -H\}$. We introduce $\mathbf{Z}^{j,bl}$, $j = 1,2$, satisfying

$$\begin{cases} \text{div}_y\ \mathbf{Z}^{j,bl} = q_1^{j,bl} \quad \text{in } Z^-; \\ \left[\mathbf{Z}^{j,bl}\right]_S = -(\displaystyle\int_{Z^-} q_1^{j,bl}\ dy)\mathbf{e}^2 \quad \text{on } S; \\ \mathbf{Z}^{j,bl} = 0 \quad \text{on } \cup_{k=1}^\infty \{\partial Y_F \setminus \partial Y - (0,k)\}, \quad \mathbf{Z}^{j,bl} \quad \text{is } y_1 - \text{periodic.} \end{cases} \tag{79}$$

After proposition 3.20 from [16], problem (76) has at least one solution $\mathbf{Z}^{j,bl} \in H^1(Z^+ \cup Z^-)^2 \cap C^\infty_{loc}(Z^+ \cup Z^-)^2$. Furthermore, $\mathbf{Z}^{j,bl} \in W^{1,q}((0,1)^2)^2$ and $\mathbf{Z}^{j,bl} \in W^{1,q}(Y-(0,1))^2$, $\forall q \in [1,\infty)$. Furthermore, there is $\gamma_0 > 0$ such that $e^{\gamma_0|y_2|}\mathbf{Z}^{j,bl} \in H^1(Z^+ \cup Z^-)^2$. Note that $\int_{Z^-} q_2^{j,bl}\ dy = 0$, $j = 1,2$. Next we set

$$\mathbf{Z}^{j,bl,\varepsilon}(x) = \varepsilon \mathbf{Z}^{j,bl}(\frac{x_1}{\varepsilon}, -\frac{x_2 + H}{\varepsilon}), \quad x \in \Omega^\varepsilon.$$

Now we introduce new velocity-pressure error functions by

$$\mathbf{U}^{2,\varepsilon} = \mathbf{U}^{1,\varepsilon} - H(-x_2) \sum_{i,j=1}^{2} \gamma^{j,i,\varepsilon} \frac{\partial^2 P^D}{\partial x_i \partial x_j} - \sum_{i,j=1}^{2} \big(\gamma^{j,i,bl,\varepsilon} - \varepsilon \mathbf{C}^{j,i,bl} H(x_2)\big) \frac{\partial^2 P^D}{\partial x_i \partial x_j}|_{\Sigma}$$

$$-H(x_2)\varepsilon \mathbf{u}^{1,eff} - \varepsilon \theta^{bl}(\frac{x}{\varepsilon}) \frac{d}{dx_1} \frac{\partial P^D}{\partial x_2}|_{\Sigma} - \sum_{j=1}^{2} \frac{d}{dx_1} \frac{\partial P^D}{\partial x_j}(x_1, -H)(\mathbf{Z}^{j,bl,\varepsilon} +$$

$$\varepsilon(\int_{Z^-} q_1^{j,bl} \ dy) R_\varepsilon(\mathbf{e}^2)); \tag{80}$$

$$P^{2,\varepsilon} = P^{1,\varepsilon} - H(x_2)\varepsilon p^{1,eff} - \sum_{i,j=1}^{2} \big(\pi^{j,i,bl,\varepsilon} - C_\pi^{j,i}\big) \frac{\partial^2 P^D}{\partial x_i \partial x_j}|_{\Sigma}, \tag{81}$$

where R_ε is Tartar's restriction operator (see [33]), defined after (106).

Proposition 12. *We have* $\mathbf{U}^{2,\varepsilon} \in V_{per}(\Omega^\varepsilon)$ *and for all* $\varphi \in V_{per}(\Omega^\varepsilon)$ *we have*

$$|\int_{\Omega^\varepsilon} \nabla \mathbf{U}^{2,\varepsilon} \nabla \varphi \ dx - \int_{\Omega^\varepsilon} P^{2,\varepsilon} \ div \ \varphi \ dx| \le C \|\nabla \varphi\|_{L^2(\Omega_2^\varepsilon)^4} + \|\varphi\|_{H^1(\Omega_1)^2}, \tag{82}$$

$$\|div \, \mathbf{U}^{2,\varepsilon}\|_{L^2(\Omega^\varepsilon)} \le C\varepsilon. \tag{83}$$

Proof of proposition 12 : We prove that $\mathbf{U}^{2,\varepsilon} \in V_{per}(\Omega^\varepsilon)$ by a direct verification. Furthermore,

$$\operatorname{div} \mathbf{U}^{2,\varepsilon} = -H(-x_2) \sum_{i,j=1}^{2} \gamma^{j,i,\varepsilon} \nabla \frac{\partial^2 P^D}{\partial x_i \partial x_j} - \sum_{i,j=1}^{2} \big(\gamma_1^{j,i,bl,\varepsilon} - \varepsilon C_1^{j,i,bl} H(x_2)\big) \frac{d}{dx_1} \frac{\partial^2 P^D}{\partial x_i \partial x_j}|_{\Sigma}$$

$$-\varepsilon \theta_1^{bl}(\frac{x}{\varepsilon}) \frac{d^2}{dx_1^2} \frac{\partial P^D}{\partial x_2}|_{\Sigma} - \sum_{j=1}^{2} \frac{d^2}{dx_1^2} \frac{\partial P^D}{\partial x_j}(x_1, -H)(\mathbf{Z}_1^{j,bl,\varepsilon} + \varepsilon(\int_{Z^-} q_1^{j,bl} \ dy)(R_\varepsilon(\mathbf{e}^2))_1), \tag{84}$$

which yields (83).

It remains to estimate the right hand side and prove (82):

$$\int_{\Omega^\varepsilon} \nabla \mathbf{U}^{2,\varepsilon} \nabla \varphi - \int_{\Omega^\varepsilon} P^{2,\varepsilon} \text{ div } \varphi = \int_\Sigma \big(\sigma_0 + \varepsilon \sigma_1 + \sum_{j=1}^2 B_\varepsilon^j\big) \mathbf{e}^2 \varphi \; dS -$$

$$\int_{\{x_2=-H\}} \sum_{j=1}^2 w_1^{j,\varepsilon} \varphi_1 \frac{\partial^2 P^D}{\partial x_j \partial x_2} \; dS + \int_{\Omega_2^\varepsilon} \varphi (\sum_{j=1}^2 A_\varepsilon^j - A_\varepsilon^{22}) \; dx - 2 \int_{\Omega^\varepsilon} A_\varepsilon^{12} \nabla \varphi \; dx$$

$$- \int_{\Omega_1} (A_\varepsilon^{32} + A_\varepsilon^{42}) \varphi \; dx - 2 \int_{\Omega_2^\varepsilon} \sum_{j=1}^2 \nabla \mathbf{q}^{j,bl} (\frac{x_1}{\varepsilon}, \frac{x_2 + H}{\varepsilon}) \nabla \frac{\partial P^D}{\partial x_j} (x_1, -H) \varphi \; dx -$$

$$\int_{\Omega_2^\varepsilon} \sum_{j=1}^2 (\Delta \frac{\partial P^D}{\partial x_j} (x_1, -H) \mathbf{q}^{j,bl} (\frac{x_1}{\varepsilon}, \frac{x_2 + H}{\varepsilon}) +$$

$$\frac{1}{\varepsilon} \nabla \frac{\partial P^D}{\partial x_j} (x_1, -H) z^{j,bl} (\frac{x_1}{\varepsilon}, \frac{x_2 + H}{\varepsilon})) \varphi \; dx + \int_{\Omega_2^\varepsilon} \sum_{j,i=1}^2 A_\varepsilon^{1,j,i} \nabla \varphi \; dx +$$

$$\int_{\Omega^\varepsilon} \sum_{j,i=1}^2 A_\varepsilon^{2,j,i} \varphi \; dx + \sum_{j,i=1}^2 \int_{\Omega^\varepsilon} \{A_\varepsilon^{3,j,i} + A_\varepsilon^{4,j,i}\} \nabla \varphi \; dx - \sum_{i,j=1}^2 \int_\Sigma \big(B_\varepsilon^{1,j,i} + B_\varepsilon^{2,j,i}\big) \mathbf{e}^2 \varphi \; dS,$$

$$- \int_{\Omega^\varepsilon} \nabla (\sum_{j=1}^2 \frac{d}{dx_1} \frac{\partial P^D}{\partial x_j} (x_1, -H) (\mathbf{Z}^{j,bl,\varepsilon} + \varepsilon (\int_{Z^-} q_1^{j,bl} \; dy) R_\varepsilon (\mathbf{e}^2))) \nabla \varphi \; dx +$$

$$\int_{\Omega^\varepsilon} (\sum_{i,j=1}^2 \big(\pi^{j,i,bl,\varepsilon} - C_\pi^{j,i}\big) \frac{\partial^2 P^D}{\partial x_i \partial x_j} |_\Sigma) \text{ div } \varphi \; dx, \tag{85}$$

where

$$A_\varepsilon^{1,j,i} = -\nabla \gamma^{j,i,\varepsilon} \frac{\partial^2 P^D}{\partial x_i \partial x_j} - \gamma^{j,i,\varepsilon} \otimes \nabla \frac{\partial^2 P^D}{\partial x_i \partial x_j}, \tag{86}$$

$$A_\varepsilon^{2,j,i} = -(\gamma^{j,i,bl,\varepsilon} - \varepsilon H(x_2) \mathbf{C}^{j,i,bl}) \frac{d^2}{dx_1^2} \frac{\partial^2 P^D}{\partial x_i \partial x_j} |_\Sigma -$$

$$(\pi^{j,i,bl,\varepsilon} - C_\pi^{j,i} H(x_2)) \frac{d}{dx_1} \frac{\partial^2 P^D}{\partial x_i \partial x_j} |_\Sigma \mathbf{e}^1, \tag{87}$$

$$A_\varepsilon^{3,j,i} = -2 \{ (\gamma^{j,i,bl,\varepsilon} - \varepsilon H(x_2) \mathbf{C}^{j,i,bl}) \otimes \nabla \frac{\partial^2 P^D}{\partial x_i \partial x_j} |_\Sigma \}, \tag{88}$$

$$A_\varepsilon^{4,j,i} = -\varepsilon \nabla \theta^{bl} (\frac{x}{\varepsilon}) \frac{d}{dx_1} \frac{\partial P^D}{\partial x_2} |_\Sigma \mathbf{e}^1 - \varepsilon \theta^{bl} (\frac{x}{\varepsilon}) \otimes \nabla \frac{\partial^2 P^D}{\partial x_1 \partial x_2} |_\Sigma \tag{89}$$

$$B_\varepsilon^{1,j,i} = -\gamma^{j,i,\varepsilon}(\cdot,-0)\otimes\nabla\frac{\partial^2 P^D}{\partial x_i\partial x_j}|_\Sigma - \nabla\gamma^{j,i,\varepsilon}|_\Sigma\frac{\partial^2 P^D}{\partial x_i\partial x_j}|_\Sigma \tag{90}$$

$$B_\varepsilon^{2,j,i} = -\varepsilon\mathbf{C}^{j,i,bl}\otimes\nabla\frac{\partial^2 P^D}{\partial x_i\partial x_j}|_\Sigma. \tag{91}$$

Then

$$|\sum_{j,i=1}^{2}\int_{\Omega_2^\varepsilon} A_\varepsilon^{1,j,i}\nabla\varphi\ dx\ |\le C\varepsilon^{1/2}\|\nabla\varphi\|_{L^2(\Omega_2^\varepsilon)^4} \tag{92}$$

$$|\sum_{j,i=1}^{2}\int_{\Omega_2^\varepsilon} A_\varepsilon^{2,j,i}\varphi\ dx\ |\le C\varepsilon^{3/2}\|\nabla\varphi\|_{L^2(\Omega_2^\varepsilon)^4} \tag{93}$$

$$|\sum_{j,i=1}^{2}\int_{\Omega_1} A_\varepsilon^{2,j,i}\varphi\ dx\ |\le C\varepsilon^{1/2}\|\varphi\|_{L^2(\Omega_1)^2} \tag{94}$$

$$|\sum_{j,i=1}^{2}\int_{\Omega^\varepsilon} A_\varepsilon^{3,j,i}\nabla\varphi\ dx\ |\le C\varepsilon^{3/2}\|\nabla\varphi\|_{L^2(\Omega^\varepsilon)^4} \tag{95}$$

$$|\sum_{j,i=1}^{2}\int_{\Omega^\varepsilon} A_\varepsilon^{4,j,i}\nabla\varphi\ |\le C\varepsilon^{1/2}\|\nabla\varphi\|_{L^2(\Omega^\varepsilon)^4}. \tag{96}$$

and

$$|\sum_{j,i=1}^{2}\int_{\Sigma} B_\varepsilon^{1,j,i}\mathbf{e}^2\varphi\ dS\ |\le C\varepsilon^{1/2}\|\nabla\varphi\|_{L^2(\Omega_2^\varepsilon)^4} \tag{97}$$

$$|\sum_{j,i=1}^{2}\int_{\Sigma} B_\varepsilon^{2,j,i}\mathbf{e}^2\varphi\ dS\ |\le C\varepsilon^{3/2}\|\nabla\varphi\|_{L^2(\Omega_2^\varepsilon)^4}. \tag{98}$$

Proposition 12 is proved. ∎

Corollary 13. *We have*

$$\int_{\Omega^\varepsilon}|\nabla\mathbf{U}^{2,\varepsilon}|^2\ dx \le C\varepsilon||P^{2,\varepsilon}||_{L^2(\Omega^\varepsilon)} + C\|\nabla\mathbf{U}^{2,\varepsilon}\|_{L^2(\Omega_2^\varepsilon)^4} + \|\mathbf{U}^{2,\varepsilon}\|_{H^1(\Omega_1)^2}, \tag{99}$$

Hence at this point we need to estimate the pressure error $P^{2,\varepsilon}$ using the velocity error $\mathbf{U}^{2,\varepsilon}$.

4.5. Pressure estimates

Following [16] we consider the Stokes system

$$-\Delta \mathbf{a}^\varepsilon + \nabla \zeta^\varepsilon = \mathbf{M}^1_\varepsilon + \text{ div } M^2_\varepsilon \quad \text{ in } \Omega^\varepsilon; \tag{100}$$

$$\text{div } \mathbf{a}^\varepsilon = 0 \quad \text{ in } \Omega^\varepsilon; \tag{101}$$

$$\mathbf{a}^\varepsilon = 0 \quad \text{ on } \partial\Omega^\varepsilon \setminus \partial\Omega \quad \text{and on} \quad \{x_2 = h\}; \tag{102}$$

$$a^\varepsilon_2 = 0 \quad \text{and} \quad \frac{\partial a^\varepsilon_1}{\partial x_2} = G^\varepsilon \quad \text{ on } \{x_2 = -H\}; \tag{103}$$

$$\{\mathbf{a}^\varepsilon, \zeta^\varepsilon\} \quad \text{ is } L-\text{periodic in } x_1; \tag{104}$$

$$[\mathbf{a}^\varepsilon]_\Sigma = 0 \quad \text{and} \quad [(\nabla \mathbf{a}^\varepsilon - \zeta^\varepsilon I)\mathbf{e}^2]_\Sigma = G^\varepsilon_\Sigma. \tag{105}$$

We have

$$\int_{\Omega^\varepsilon} \zeta^\varepsilon \text{ div } \varphi \, dx = \int_{\Omega^\varepsilon} \nabla \mathbf{a}^\varepsilon \nabla \varphi \, dx - \int_{\Omega^\varepsilon} \mathbf{M}^1_\varepsilon \varphi \, dx + \int_{\Omega^\varepsilon} M^2_\varepsilon \nabla \varphi \, dx +$$
$$\int_\Sigma G^\varepsilon_\Sigma \varphi \, dS + \int_{\{x_2=-H\}} G^\varepsilon \varphi \, dS, \qquad \forall \varphi \in V(\Omega^\varepsilon),$$

which yields

$$| \int_{\Omega^\varepsilon} \zeta^\varepsilon \text{ div } \varphi \, dx| \leq C \Big\{ \|\nabla \mathbf{a}^\varepsilon\|_{L^2(\Omega^\varepsilon)^4} + ||\mathbf{M}^1_\varepsilon||_{L^2(\Omega_1)^2} + \varepsilon ||\mathbf{M}^1_\varepsilon||_{L^2(\Omega^\varepsilon_2)^2} + ||M^2_\varepsilon||_{L^2(\Omega^\varepsilon)^4}$$
$$+ \sqrt{\varepsilon} \Big(||G^\varepsilon_\Sigma||_{L^2(\Sigma)} + ||G^\varepsilon||_{L^2(\{x_2=-H\})} \Big) \Big\} ||\nabla \varphi||_{L^2(\Omega^\varepsilon)^4}. \tag{106}$$

At this point we need Tartar's restriction operator R_ε (see [1], [32] and [33]). It is constructed for every pore on the following way:

Let γ be a smooth curve, strictly contained in the cell Y, and enclosing the solid part Y_s. Let Y_M be the domain between γ and ∂Y_s. Then using an intermediary nonhomogeneous Stokes system in Y_M a linear operator $R : H^1(Y)^2 \to H^1(Y_F)^2$ is constructed, such that

$$R\mathbf{u}(y) = \mathbf{u}(y) \quad \text{for} \quad y \in Y \setminus (\bar{Y}_s \cup Y_M), \quad R\mathbf{u}(y) = 0 \quad \text{for} \quad y \in Y_s,$$
$$\mathbf{u} = 0 \text{ on } Y_s \quad \Rightarrow R\mathbf{u} = \mathbf{u} \quad \text{on} \quad Y, \quad \text{div } \mathbf{u} = 0 \text{ on } Y \quad \Rightarrow \text{div } (R\mathbf{u}) = 0 \quad \text{on} \quad Y,$$
$$||R\mathbf{u}||_{H^1(Y_F)^2} \leq C||\mathbf{u}||_{H^1(Y)^2}, \quad \forall \mathbf{u} \in H^1(Y)^2.$$

Next the operator $R_\varepsilon : H^1(\Omega)^2 \to H^1(\Omega^\varepsilon)^2$ is defined by applying the operator R

to each $\varepsilon(Y+k)$ cell. After [1], [32] and [33], we have

$$
\begin{aligned}
R_\varepsilon \mathbf{u}(x) = 0 \quad \text{for} \quad x \in \Omega \setminus \Omega^\varepsilon, \quad \mathbf{u} = 0 \ \text{ on } \Omega \setminus \Omega^\varepsilon \ \Rightarrow R_\varepsilon \mathbf{u} = \mathbf{u} \quad \text{on} \quad \Omega^\varepsilon, \\
\text{div } \mathbf{u} = 0 \ \text{ on } \Omega \quad \Rightarrow \text{div } (R_\varepsilon \mathbf{u}) = 0 \quad \text{on} \quad \Omega^\varepsilon, \\
||R_\varepsilon \mathbf{u}||_{L^2(\Omega^\varepsilon)^2} \leq C||\mathbf{u}||_{L^2(\Omega)^2} + C\varepsilon||\nabla \mathbf{u}||_{L^2(\Omega)^4}, \quad \forall \mathbf{u} \in H^1(\Omega)^2, \qquad (107) \\
||\nabla R_\varepsilon \mathbf{u}||_{L^2(\Omega^\varepsilon)^2} \leq \frac{C}{\varepsilon}||\mathbf{u}||_{L^2(\Omega)^2} + C||\nabla \mathbf{u}||_{L^2(\Omega)^4}, \quad \forall \mathbf{u} \in H^1(\Omega)^2. \qquad (108)
\end{aligned}
$$

Next we extend ζ^ε to $\tilde{\zeta}^\varepsilon$ using formula (17), proposed by Lipton and Avellaneda.

The calculation of Lipton and Avellaneda gives

$$
\int_\Omega \tilde{\zeta}^\varepsilon \text{ div } \varphi \ dx = \int_{\Omega^\varepsilon} \zeta^\varepsilon \text{ div } (R_\varepsilon \varphi) \ dx, \quad \forall \varphi \in V(\Omega^\varepsilon). \qquad (109)
$$

Proposition 14. *We have*

$$
\begin{aligned}
||\tilde{\zeta}^\varepsilon||_{L^2(\Omega)} \leq \frac{C}{\varepsilon}\Bigg\{ \|\nabla \mathbf{a}^\varepsilon\|_{L^2(\Omega^\varepsilon)^4} + ||\mathbf{M}^1_\varepsilon||_{L^2(\Omega_1)^2} + \varepsilon||\mathbf{M}^1_\varepsilon||_{L^2(\Omega^\varepsilon_2)^2} + ||M^2_\varepsilon||_{L^2(\Omega^\varepsilon)^4} \\
+\sqrt{\varepsilon}\Big(||G^\varepsilon_\Sigma||_{L^2(\Sigma)} + ||G^\varepsilon||_{L^2(\{x_2=-H\})} \Big) \Bigg\}. \qquad (110)
\end{aligned}
$$

Proof of proposition 14: Let $g \in L^2(\Omega)$. We set $h = g - \dfrac{1}{|\Omega|}\displaystyle\int_\Omega g \ dx$. Obviously $\int_\Omega h \ dx = 0$. Let

$$
\begin{aligned}
V_{per}(\Omega) = \{\mathbf{z} \in H^1(\Omega)^2 : \mathbf{z} = 0 \quad \text{on} \quad \{x_2 = h\}, \ z_2 = 0 \quad \text{on} \quad \{x_2 = -H\} \\
\text{and } \mathbf{z} \text{ is L-periodic in } x_1 \text{ variable } \}. \qquad (111)
\end{aligned}
$$

Then there exists $\varphi \in V_{per}(\Omega)$ such that div $\varphi = h$ in Ω and $||\varphi||_{H^1(\Omega)^2} \leq C||h||_{L^2(\Omega)}$, for all $h \in L^2_0(\Omega)$.

Therefore we have

$$
\int_\Omega \tilde{\zeta}^\varepsilon h \ dx = \int_\Omega \tilde{\zeta}^\varepsilon \text{ div } \varphi \ dx = \int_{\Omega^\varepsilon} \zeta^\varepsilon \text{ div } (R_\varepsilon \varphi) \ dx
$$

and using (106) and (107), (108) yields

$$
\begin{aligned}
|\int_\Omega \tilde{\zeta}^\varepsilon \ h \ dx| \leq \frac{C}{\varepsilon}\Bigg\{ ||\nabla \mathbf{a}^\varepsilon||_{L^2(\Omega^\varepsilon)^4} + ||\mathbf{M}^1_\varepsilon||_{L^2(\Omega_1)^2} + \varepsilon||\mathbf{M}^1_\varepsilon||_{L^2(\Omega^\varepsilon_2)^2} + ||M^2_\varepsilon||_{L^2(\Omega^\varepsilon)^4} \\
+\sqrt{\varepsilon}\Big(||G^\varepsilon_\Sigma||_{L^2(\Sigma)} + ||G^\varepsilon||_{L^2(\{x_2=-H\})} \Big) \Bigg\} ||\nabla \varphi||_{L^2(\Omega)^4}. \qquad (112)
\end{aligned}
$$

Since

$$\int_{\Omega}(\tilde{\zeta}^{\varepsilon}-\frac{1}{|\Omega|}\int_{\Omega}\tilde{\zeta}^{\varepsilon}\ dy)g\ dx=\int_{\Omega}(\tilde{\zeta}^{\varepsilon}-\frac{1}{|\Omega|}\int_{\Omega}\tilde{\zeta}^{\varepsilon}\ dy)h\ dx=\int_{\Omega}\tilde{\zeta}^{\varepsilon}h\ dx,$$

we conclude that $\tilde{\zeta}^{\varepsilon}-\frac{1}{|\Omega|}\int_{\Omega}\tilde{\zeta}^{\varepsilon}\ dy$ satisfies bound (110).

For the mean we have

$$0=\int_{\Omega_1}\tilde{\zeta}^{\varepsilon}\ dx=\int_{\Omega_1}(\tilde{\zeta}^{\varepsilon}-\frac{1}{|\Omega|}\int_{\Omega}\tilde{\zeta}^{\varepsilon}\ dy)\ dx+\int_{\Omega}\frac{|\Omega_1|}{|\Omega|}\tilde{\zeta}^{\varepsilon}\ dx$$

and

$$|\frac{1}{|\Omega|}\int_{\Omega}\tilde{\zeta}^{\varepsilon}\ dx|\leq\frac{1}{|\Omega|^{1/2}}||\tilde{\zeta}^{\varepsilon}-\frac{1}{|\Omega|}\int_{\Omega}\tilde{\zeta}^{\varepsilon}\ dy||_{L^2(\Omega_1)^2}. \tag{113}$$

Estimate (113) implies bound (110) for $\tilde{\zeta}^{\varepsilon}$. ∎

4.6. Global energy estimate and proof of theorem 1

Proof of theorem 1: Now we choose $\varphi=\mathbf{U}^{2,\varepsilon}$ as test function in (85). Using estimates (92) - (98) and estimate (110) from proposition 14, we obtain

$$\begin{aligned}|\int_{\Omega^{\varepsilon}}\nabla\mathbf{U}^{2,\varepsilon}\nabla\mathbf{U}^{2,\varepsilon}\ |\leq\frac{C}{\varepsilon}\{\|\nabla\mathbf{U}^{2,\varepsilon}\|_{L^2(\Omega_2^{\varepsilon})^4}+C\}\|\ \mathrm{div}\ \ \mathbf{U}^{2,\varepsilon}\|_{L^2(\Omega_2^{\varepsilon})}+\\ C\|\nabla\mathbf{U}^{2,\varepsilon}\|_{L^2(\Omega_2^{\varepsilon})^4},\end{aligned} \tag{114}$$

which yields

$$||\nabla\mathbf{U}^{2,\varepsilon}||_{L^2(\Omega^{\varepsilon})^4}\leq C, \tag{115}$$

$$||\ \mathrm{div}\ \mathbf{U}^{2,\varepsilon}||_{L^2(\Omega^{\varepsilon})^4}+||\mathbf{U}^{2,\varepsilon}||_{L^2(\Omega_2^{\varepsilon})^2}\leq C\varepsilon \tag{116}$$

$$||P^{2,\varepsilon}||_{L^2(\Omega^{\varepsilon})}\leq\frac{C}{\varepsilon} \tag{117}$$

Hence estimates (20)-(21) are proved.

It remains to prove estimates (18)-(19).

First (115)-(116) imply

$$||\mathbf{U}^{2,\varepsilon}||_{L^2(\Sigma)^2}\leq C\sqrt{\varepsilon} \tag{118}$$

and estimate (19) is proved.

Next we remark that in Ω_1 the error functions $\mathbf{U}^{2,\varepsilon}$ and $P^{2,\varepsilon}$ satisfy the system

$$\begin{cases} -\Delta \mathbf{U}^{2,\varepsilon} + \nabla P^{2,\varepsilon} = \mathbf{G}^{1,\varepsilon} + \ \mathrm{div}\ G^{2,\varepsilon} \quad \text{in } \Omega_1; \\ \mathrm{div}\ \mathbf{U}^{2,\varepsilon} = \Lambda^\varepsilon \quad \text{in } \ \Omega_1; \\ \mathbf{U}^{2,\varepsilon} = \xi^\varepsilon \quad \text{on } \ \Sigma; \quad \mathbf{U}^{2,\varepsilon} = 0 \quad \text{on } \ \{x_2 = h\}; \\ \{\mathbf{U}^{2,\varepsilon}, P^{2,\varepsilon}\} \quad \text{is } L\text{-periodic in } \ x_1, \end{cases} \tag{119}$$

where, after neglecting the boundary layer tails,

$$\Lambda^\varepsilon = -\sum_{i,j=1}^{2} \big(\gamma_1^{j,i,bl,\varepsilon} - \varepsilon C_1^{j,i,bl}\big) \frac{d}{dx_1} \frac{\partial^2 P^D}{\partial x_i \partial x_j}|_\Sigma - \varepsilon \theta_1^{bl}(\frac{x}{\varepsilon}) \frac{d^2}{dx_1^2} \frac{\partial P^D}{\partial x_2}|_\Sigma \tag{120}$$

$$\mathbf{G}^{1,\varepsilon} = (\frac{Q^{2,\varepsilon}}{\varepsilon}\mathbf{e}^1 + \beta^{2,bl,\varepsilon} - C_1^{2,bl}\mathbf{e}^1) \frac{d^2}{dx_1^2}(\frac{\partial P^D}{\partial x_2}|_\Sigma) + \sum_{j,i=1}^{2} A_\varepsilon^{2,j,i}, \tag{121}$$

$$G^{2,\varepsilon} = \frac{d}{dx_1}(\frac{\partial P^D}{\partial x_2}|_\Sigma)\mathbf{e}^1 \otimes (2\beta^{2,bl,\varepsilon} - 2C_1^{2,bl}\mathbf{e}^1 - \frac{Q^{2,\varepsilon}}{\varepsilon}\mathbf{e}^1) + \sum_{j,i=1}^{2} (A_\varepsilon^{3,j,i} + A_\varepsilon^{4,j,i}). \tag{122}$$

The function $Q^{2,\varepsilon}$ is given by (56) and, for $i, j = 1, 2$, $A_\varepsilon^{2,j,i}$, $A_\varepsilon^{3,j,i}$ and $A_\varepsilon^{4,j,i}$ by (87)-(89).

After (84), we have $||\Lambda^\varepsilon||_{L^2(\Omega_1)} \leq C\varepsilon^{3/2}$. Using the basic theory of the Stokes system (see e.g. [34]) there exists $\{\mathbf{b}, \kappa\} \in H^1(\Omega_1)^2 \times L^2(\Omega_1)$, such that

$$\begin{cases} -\Delta \mathbf{b} + \nabla \kappa = 0 \quad \text{in } \Omega_1; \\ \mathrm{div}\ \mathbf{b} = \Lambda^\varepsilon \quad \text{in } \ \Omega_1; \\ \mathbf{b} \quad \text{is given on } \ \Sigma_T = \Sigma \cup \{x_2 = h\} \quad \text{and} \quad ||\mathbf{b}||_{H^{1/2}(\Sigma_T)^2} \leq C\varepsilon^{3/2}; \\ \{\mathbf{b}, \kappa\} \quad \text{is } L\text{-periodic in } \ x_1, \end{cases} \tag{123}$$

Now we see that the pair $\{\mathbf{U}^{2,\varepsilon} - \mathbf{b}, P^{2,\varepsilon} - \kappa\}$ satisfies system (119) with $\Lambda^\varepsilon = 0$. Such system admits the notion of a very weak solution, introduced by transposition. We refer to [9] , pages 61-68, and [25] for the definition and properties of a very weak solution. Note that $\int_\Sigma (\xi_2^\varepsilon - b_2)\ dS = 0$.

Let $H_p^k(\Omega_1)^2 = \{\mathbf{z} \in H^k(\Omega_1)^2 \mid \mathbf{z} \text{ is L-periodic and } \mathbf{z} = 0 \text{ on } \{x_2 = h\}\ \}$, $k = 1, 2$. Then the $q = r = 2$-version of proposition 4.2., page 302, from [25], gives the estimate

$$||\mathbf{U}^{2,\varepsilon} - \mathbf{b}||_{L^2(\Omega_1)^2} \leq C\{||\mathbf{G}^{1,\varepsilon}||_{(H_p^2(\Omega_1)^2)'} + ||G^{2,\varepsilon}||_{(H_p^1(\Omega_1)^4)'} + ||\xi^\varepsilon - \mathbf{b}||_{L^2(\Sigma_T)^2}\} \tag{124}$$

Using estimates (52), (54) and (94)-(96), choosing $Q^{2,\varepsilon}$ with zero mean and repeating calculations analogous to ones from (58) to other terms, yield

$$||\mathbf{G}^{1,\varepsilon}||_{(H^1_p(\Omega_1)^2)'} + ||G^{2,\varepsilon}||_{(H^1_p(\Omega_1)^4)'} \leq C\varepsilon^{3/2}. \tag{125}$$

Now we are able to conclude that

$$||\mathbf{U}^{2,\varepsilon}||_{L^2(\Omega_1)^2} \leq C\sqrt{\varepsilon} \tag{126}$$

and estimate (18) is proved. ∎

5. Proof of theorem 2

The proof is in fact a slight modification of the proof of theorem 1. Our goal is to gain a $\sqrt{\varepsilon}$ in estimate (115).

By inspecting the proof of proposition 5, we find out that the origin of the "bad" estimate is the term $\varepsilon^{-1}\pi^{j,\varepsilon}\nabla\dfrac{\partial P^D}{\partial x_j}$ in (37). So we have to correct it in Ω_2^ε. Next, the same type of difficulty arises with the term $\varepsilon^{-1}C_\pi^2\dfrac{d}{dx_1}(\dfrac{\partial P^D}{\partial x_2}|_\Sigma)H(-x_2)$ in (47). We handle it by modifying $\{\mathbf{U}^\varepsilon, P^\varepsilon\}$. We include into the new velocity-pressure error pair the correction for the pressure term in (37). The constant C_π^2 corresponds to the behavior of $\omega^{2,bl}$ for $y_2 > 0$ and we erase it in Ω_2^ε. Erasing it creates a pressure jump of order $O(\varepsilon^{-1})$ and we compensate it by introducing a Darcy pressure field of such order in Ω_2.

We start by introducing an auxiliary problem correcting the singular pressure in (47):

$$\begin{cases} -\Delta_y \mathbf{w}_\pi^{i,k}(y) + \nabla_y \kappa_\pi^{i,k}(y) = \pi^i(y)\mathbf{e}^k & \text{in } Y_F \\ \operatorname{div}_y \mathbf{w}_\pi^{i,k}(y) = 0 & \text{in } Y_F \\ \mathbf{w}_\pi^{i,k}(y) = 0 & \text{on } (\partial Y_F \setminus \partial Y) \end{cases} \tag{127}$$

where π^i is given by (6) and $\int_{Y_F} \kappa_\pi^{i,k}(y)\, dy = 0$.

Modified $\{\mathbf{U}^\varepsilon, P^\varepsilon\}$ now read

$$\tilde{\mathbf{U}}^\varepsilon = \mathbf{v}^\varepsilon - H(x_2)(\mathbf{u}^{eff} - \mathbf{e}^1 C_1^{2,bl} \frac{\partial P^D}{\partial x_2}|_\Sigma) + H(-x_2)\{\sum_{j=1}^2 \mathbf{w}^{j,\varepsilon} \frac{\partial P^D}{\partial x_j} -$$

$$\varepsilon C_\pi^2 \mathbf{w}^{1,\varepsilon} \frac{d}{dx_1} \frac{\partial P^D}{\partial x_2}|_\Sigma - \varepsilon \sum_{j,k=1}^2 \mathbf{w}_\pi^{j,k}(\frac{x}{\varepsilon}) \frac{\partial^2 P^D}{\partial x_j \partial x_k}\} - \beta^{2,bl,\varepsilon} \frac{\partial P^D}{\partial x_2}|_\Sigma; \tag{128}$$

$$\hat{P}^\varepsilon = p^\varepsilon - H(x_2)p^{eff} - H(-x_2)\{\varepsilon^{-2} P^D - \varepsilon^{-1}(C_\pi^2 \frac{\partial P^D}{\partial x_2}|_\Sigma + \sum_{j=1}^2 \pi^{j,\varepsilon} \frac{\partial P^D}{\partial x_j}) +$$

$$C_\pi^2 \pi^{1,\varepsilon} \frac{d}{dx_1} \frac{\partial P^D}{\partial x_2}|_\Sigma + \sum_{j,k=1}^2 \kappa_\pi^{j,k}(\frac{x}{\varepsilon}) \frac{\partial^2 P^D}{\partial x_j \partial x_k})\} - \varepsilon^{-1}(\omega^{2,bl,\varepsilon} - C_\pi^2 H(x_2)) \frac{\partial P^D}{\partial x_2}|_\Sigma. \tag{129}$$

Now all force-type terms are estimated as $C\sqrt{\varepsilon}\|\varphi\|_{H^1(\Omega^\varepsilon)^2}$. Furthermore, all normal stress jumps are of order $O(1)$.

Continuity of traces fails, but we correct it on the same way as in the original construction in subsection 4.2. The correction is of the order $O(\varepsilon^{3/2})$ in L^2 for the velocity and of order $O(\sqrt{\varepsilon})$ in L^2 for the pressure and does not contribute to the result. Next we correct the effects on the boundary $\{x_2 = -H\}$ and the compressibility effects. They are all of the next order and do not contribute to result.

The calculations yield the following estimates

$$||\nabla \tilde{\mathbf{U}}^{2,\varepsilon}||_{L^2(\Omega^\varepsilon)^4} \le C\sqrt{\varepsilon}, \tag{130}$$

$$||\ \mathrm{div}\ \tilde{\mathbf{U}}^{2,\varepsilon}||_{L^2(\Omega^\varepsilon)^4} \le C\varepsilon \tag{131}$$

$$||\tilde{\mathbf{U}}^{2,\varepsilon}||_{L^2(\Omega_2^\varepsilon)^2} \le C\varepsilon^{3/2} \tag{132}$$

$$||\hat{P}^{2,\varepsilon}||_{L^2(\Omega^\varepsilon)} \le \frac{C}{\sqrt{\varepsilon}} \tag{133}$$

Now (130)-(132) imply

$$||\tilde{\mathbf{U}}^{2,\varepsilon}||_{L^2(\Sigma)^2} \le C\varepsilon \tag{134}$$

The rest of the proof is identical to the proof of theorem 1. Only difference is that we have gained a $\sqrt{\varepsilon}$ in the estimates. ∎

References

[1] G.Allaire, One-Phase Newtonian Flow, in "Homogenization and Porous Media", ed. U.Hornung, Springer, New-York, 1997, p. 45-68.

[2] W. Bangerth and R. Hartmann and G. Kanschat, deal.II – a General Purpose Object Oriented Finite Element Library, ACM Trans. Math. Softw., 2007, 33, 24/1–24/27, 4.

[3] G.S. Beavers, D.D. Joseph, Boundary conditions at a naturally permeable wall, J. Fluid Mech., 30 (1967) 197-207.

[4] Becker, R. and Rannacher,R., An optimal control approach to a posteriori error estimation in finite element methods, Acta Numerica, 10(2001) 1–102.

[5] Brenner, S. C. and Scott, L.R, 2002, The mathematical theory of finite element methods, second edition, Texts in Applied Mathematics, Springer-Verlag.

[6] Brezzi, F. and Fortin, M., Mixed and hybrid finite element methods, 1991, Springer-Verlag New York, Inc., New York, NY, USA.

[7] T. Carraro, C. Goll, A. Marciniak-Czochra, A. Mikelić, Pressure jump interface law for the Stokes-Darcy coupling: Confirmation by direct numerical simulations, Journal of Fluid Mechanics, 732 (2013) 510-536.

[8] Ciarlet, P. G., Finite Element Method for Elliptic Problems, 2002, Society for Industrial and Applied Mathematics, Philadelphia, PA, USA.

[9] C. Conca, Étude d'un fluide traversant une paroi perforée I. Comportement limite près de la paroi, J. Math. pures et appl., 66 (1987) 1-44. II. Comportement limite loin de la paroi, J. Math. pures et appl., 66 (1987) 45-69.

[10] M. Discacciati, E. Miglio, A. Quarteroni, Mathematical and numerical models for coupling surface and groundwater flows, Appl. Numer. Math., 43 (2002) 57–74.

[11] M. Discacciati, A. Quarteroni, Navier-Stokes/Darcy Coupling: Modeling, Analysis, and Numerical Approximation, Rev. Mat. Complut., 22 (2009) 315-426.

[12] C. Goll and T. Wick and W. Wollner, DOpElib: Differential Equations and Optimization Environment; A Goal Oriented Software Library for Solving PDEs and Optimization Problems with PDEs, 2012, *submitted,* `www.dopelib.net`

[13] N. S. Hanspal, A. N. Waghode, V. Nassehi, R. J. Wakeman, Numerical Analysis of Coupled Stokes/Darcy Flows in Industrial Filtrations, Transport in Porous Media, 64 (2006) 73-101.

[14] O. Iliev, V. Laptev, On Numerical Simulation of Flow Through Oil Filters, Computing and Visualization in Science, 6 (2004) 139-146.

[15] A.S. Jackson, I. Rybak, R. Helmig, W.G. Gray, C.T. Miller, Thermodynamically constrained averaging theory approach for modeling flow and transport phenomena in porous medium systems: 9. Transition region models, Advances in Water Resources, 42 (2012) 71-90.

[16] W.Jäger, A.Mikelić, On the Boundary Conditions at the Contact Interface between a Porous Medium and a Free Fluid, Ann. Sc. Norm. Super. Pisa, Cl. Sci. - Ser. IV, XXIII (1996) 403 - 465.

[17] W. Jäger, A. Mikelić, On the interface boundary conditions by Beavers, Joseph and Saffman, SIAM J. Appl. Math., 60(2000) 1111-1127.

[18] W. Jäger, A. Mikelić , N. Neuß, Asymptotic analysis of the laminar viscous flow over a porous bed, SIAM J. on Scientific and Statistical Computing, 22 (2001) 2006 - 2028.

[19] W. Jäger, A. Mikelić, Modeling effective interface laws for transport phenomena between an unconfined fluid and a porous medium using homogenization, Transport in Porous Media, 78 (2009) 489-508.

[20] M. Kaviany: Principles of heat transfer in porous media, Springer-Verlag New York Inc., 2nd Revised edition, 1995.

[21] R.E. Larson, J.J.L. Higdon, Microscopic flow near the surface of two-dimensional porous media. Part I. Axial flow, J. Fluid Mech. , 166 (1986), 449 - 472. Microscopic flow near the surface of two-dimensional porous media. Part II. Transverse flow, J. Fluid Mech., 178 (1986) 119 - 136.

[22] W. J. Layton, F. Schieweck, I. Yotov, Coupling fluid flow with porous media flow, SIAM Journal on Numerical Analysis, 40 (2002) 2195-2218.

[23] T. Levy, E. Sanchez-Palencia, On boundary conditions for fluid flow in porous media, International Journal of Engineering Science, 13 (1975) 923-940.

[24] R. Lipton, M. Avellaneda, A Darcy Law for Slow Viscous Flow Past a Stationary Array of Bubbles, Proc. Royal Soc. Edinburgh, 114A (1990) 71-79.

[25] A. Marciniak-Czochra, A. Mikelić, Effective pressure interface law for transport phenomena between an unconfined fluid and a porous medium using homogenization, SIAM: Multiscale modeling and simulation, 10 (2012) 285-305.

[26] V. Nassehi, N.S. Hanspal, A.N. Waghode, W.R. Ruziwa, R.J. Wakeman, Finite-element modelling of combined free/porous flow regimes: simulation of flow through pleated cartridge filters, Chemical Engineering Science, 60 (2005) 995-1006.

[27] D.A. Nield, The Beavers-Joseph boundary condition and related matters: A historical and critical note, Transp Porous Med, Vol. 78 (2009) 537-540.

[28] J.A. Ochoa-Tapia, S. Whitaker, Momentum transfer at the boundary between a porous medium and a homogeneous fluid - I. Theoretical development; II. Comparison with experiment, Int. J. Heat Mass Transfer, 38 (1995) 2635-2646 and 2647-2655.

[29] B. Rivière, I. Yotov, Locally conservative coupling of Stokes and Darcy flows, SIAM Journal on Numerical Analysis, 42 (2005) 1959-1977.

[30] P.G. Saffman, On the boundary condition at the interface of a porous medium, Studies in Applied Mathematics, 1 (1971), p. 93-101.

[31] M. Sahraoui, M. Kaviany, Slip and no-slip velocity boundary conditions at interface of porous, plain media, Int. J. Heat Mass Transfer, 35 (1992) 927-943.

[32] E. Sanchez-Palencia, Non-Homogeneous Media and Vibration Theory, Lecture Notes in Physics, 127, Springer Verlag, 1980.

[33] L. Tartar, Convergence of the Homogenization Process, Appendix of [32].

[34] R. Temam, Navier-Stokes Equations, 3rd (revised) edition, Elsevier Science Publishers, Amsterdam, 1984.

[35] P. Yu, T.S.Lee,Y.Zeng, H. T. Low, A numerical method for flows in porous and homogenous fluid domains coupled at the interface by stress jump, Int. J. Numer. Meth. Fluids, 53 (2007) 1755–1775.